大阪大學

Oct. 19, 2012
@Grenoble

Observation of Spin-chiral Domains in Multiferroic Hexaferrites by Scanning Resonant X-ray Microdiffraction

- Study of Magnetoelectric Effects due to Multi-spin Variables -

Tsuyoshi Kimura

Graduate School of Engineering Science, Osaka University

Collaborators

Osaka Univ. Y. Yamaguchi, Y. Hiraoka, T. Ishikura, K. Okumura, Y. Kitagawa
H. Nakamura, Y. Wakabayashi

Spring-8, RIKEN Y. Tanaka, S. Shin (Scanning Resonant X-ray diffraction)

Nagoya Institute of Tech. T. Asaka (Electron diffraction, TEM)

ISSP, Univ. of Tokyo M. Soda (Neutron diffraction)

Outline

1. Introduction: Magnetoelectric effect & multi-spin variables

2. Room-temperature magnetoelectrics possibly by spin spiral

Hexaferrites $Sr_3Co_2Fe_{24}O_{41}$ with the Z-type structure

3. Observation of Spin-chiral Domains in Multiferroic Hexaferrites by Scanning Resonant X-ray

Hexaferrites $Ba_{0.5}Sr_{1.5}Zn_2Fe_{12}O_{22}$ with the Y-type structure

4. Magnetoelectric effect observed in a magnetically-disordered system

XY-like spin-glass $(Ni,Mn)TiO_3$ with the ilmenite structure

Magnetoelectric (ME) effect

Magnetoelectric effect ⇨ **Induction of** **Polarization** **by** **Magnetic fields** **(ME_H)**
Magnetization **Electric fields** **(ME_E)**

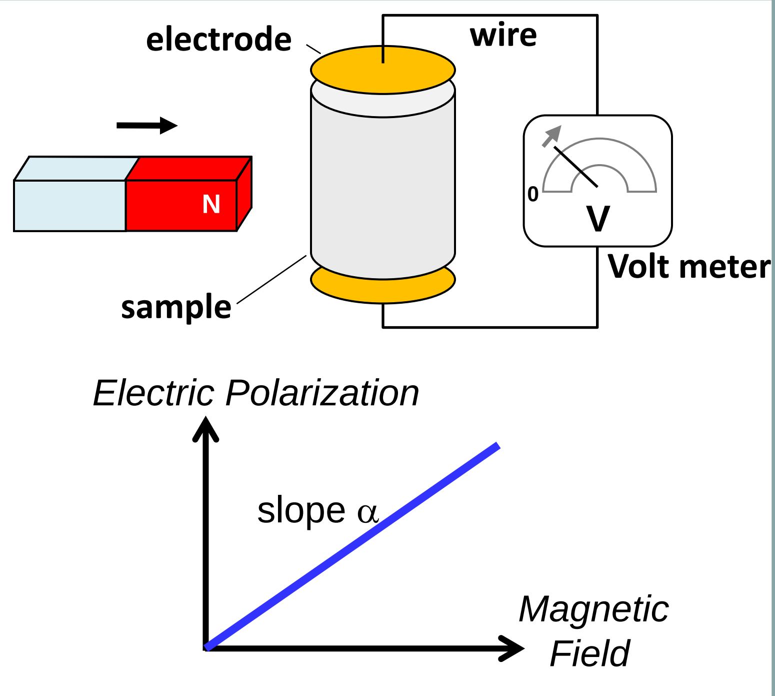

ME_H effect $P_i = \alpha_{ij} H_j$

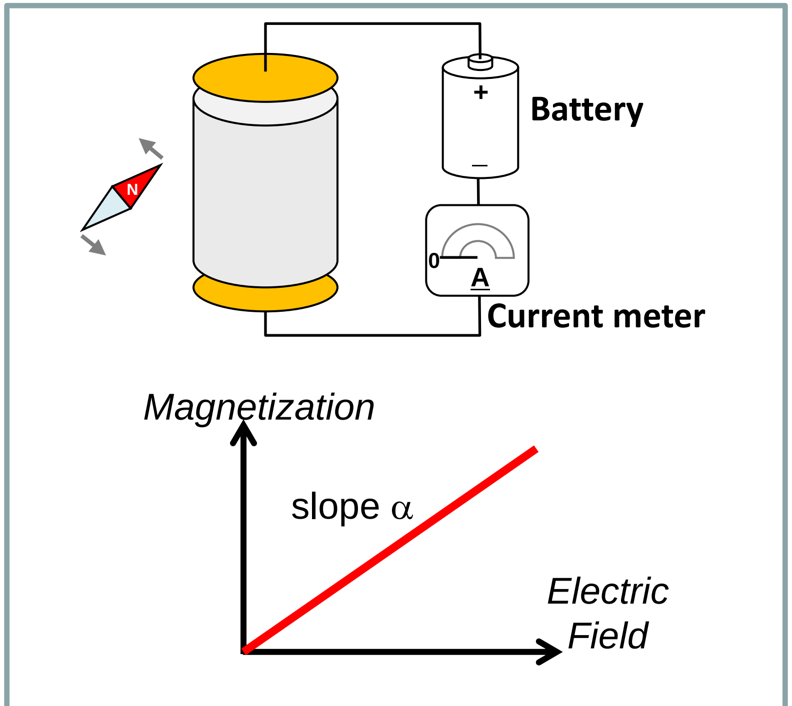

ME_E effect $M_i = \alpha_{ij} E_j$

P. Curie [1894] **First proposal of the ME effect on symmetry grounds.**
Landau & Lifshitz [1957] **Shows that the ME effect should exist in magnetic crystals.**
Dzyaloshinskii [1959] **Shows that the AF Cr_2O_3 has a magnetic symmetry which allows the effect.**
Astrov [1960] **First successful observation of the effect in a Cr_2O_3 crystal.**

Symmetry aspect is useful to explain the ME effect.

$$M_i = \alpha_{ij}E_j$$

Since E is a polar 1st rank tensor & M is an axial 1st rank tensor,
the ME effect is an axial 2nd rank tensor which transforms as follows.

e.g. inversion operation $\bar{1}$

$$\begin{pmatrix} a_{11} & a_{12} & a_{13} \\ a_{21} & a_{22} & a_{23} \\ a_{31} & a_{32} & a_{33} \end{pmatrix} = \begin{pmatrix} -1 & 0 & 0 \\ 0 & -1 & 0 \\ 0 & 0 & -1 \end{pmatrix}$$

In tensor form,

$$M'_i = \pm|a|a_{ij}M_j = \pm|a|a_{ij}\alpha_{jk}E_k$$

$$= \pm|a|a_{ij}\alpha_{jk}a_{lk}E'_l = \alpha'_{il}E'_l \Rightarrow \alpha'_{il} = \pm|a|a_{ij}\alpha_{jk}a_{lk}$$

In matrix form,

$$(M') = \pm|a|\,(a)\,(M) = \pm|a|\,(a)\,(\alpha)\,(E)$$

$$= \pm|a|\,(a)\,(\alpha)(a)_t\,(E') = (\alpha')\,(E') \Rightarrow (\alpha') = \pm|a|\,(a)(\alpha)(a)_t$$

The ME effect vanishes for all symmetry groups containing time reversal symmetry (1').

$$(\alpha') = (-1)(+1)(+1)(\alpha)(+1) = (-\alpha) = (\alpha) = 0$$

The ME effect also disappears for ordinary inversion symmetry ($\bar{1}$) *operations.*

$$(\alpha') = (+1)(-1)(-1)(\alpha)(-1) = (-\alpha) = (\alpha) = 0$$

For space inversion accompanied by time inversion ($\bar{1}'$), *the ME effect is permitted.*

$$(\alpha') = (-1)(-1)(-1)(\alpha)(-1) = (\alpha) = (\alpha)$$

Requirements of the linear ME effect $\longrightarrow$ Both space inversion symmetry & time reversal symmetry must be broken.

Constraints on appearance of linear ME effect
—Breaking of Space Inversion & Time reversal symmtries—

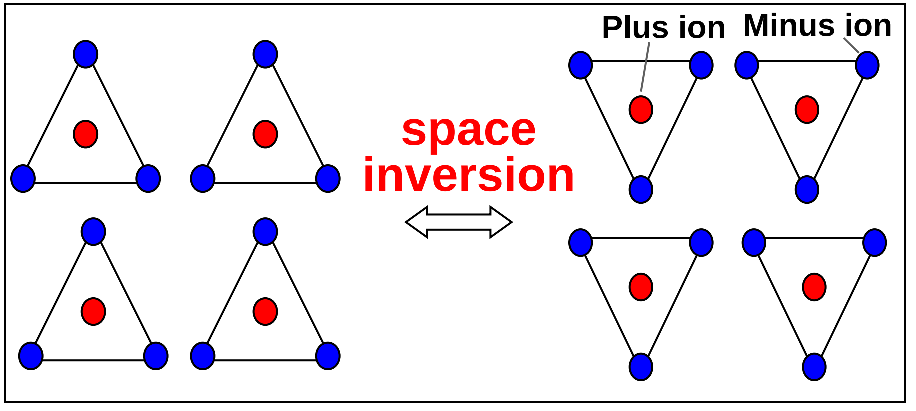

e.g., ferroelectrics

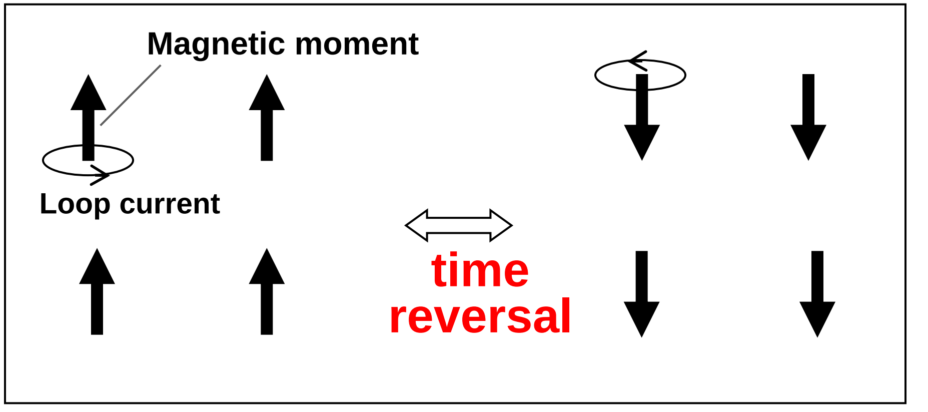

e.g., ferromagnets

Multiferroics

Broken of space inversion symmetry in spiral spin systems

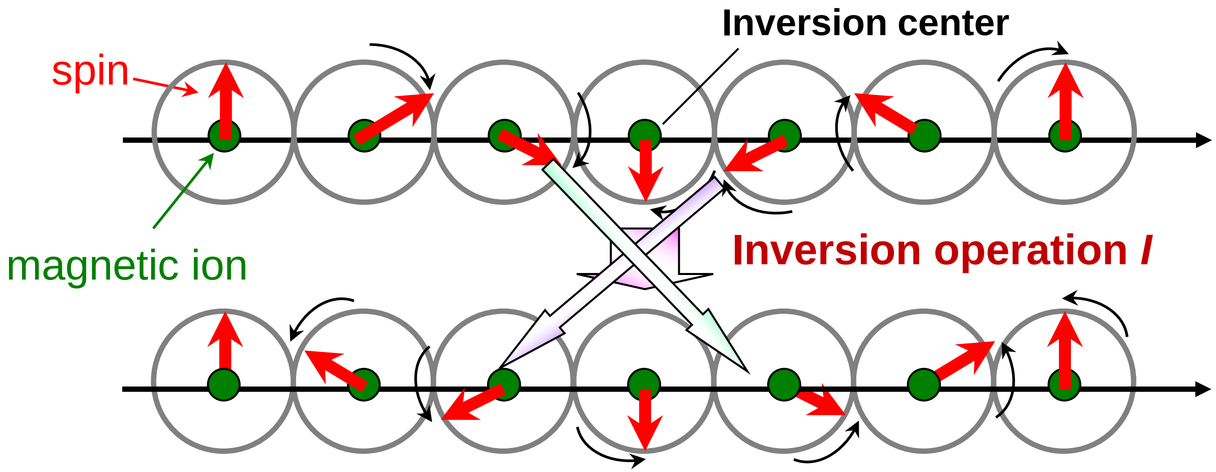

The CW & CCW spiral structures are inverted by *I* to each other.
However, these two spiral structures are not identical.

Thus, the inversion symmetry is broken by a spiral spin order.

To make system ferroelectric,

1. Cycloidal spiral structure

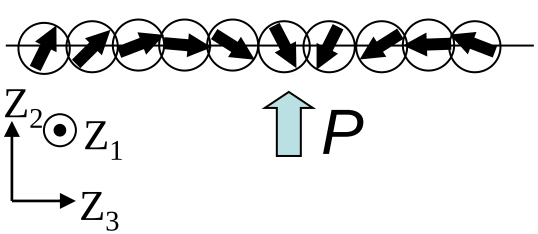

$m \perp Z_3$
$2 // Z_2$
$m' \perp Z_1$

2. Screw spiral structure + low crystal symmetry

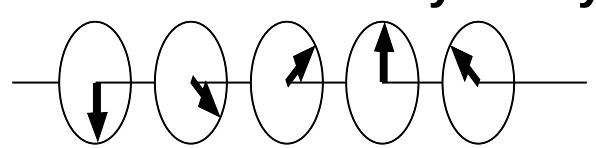

$2 \perp Z_3$

e.g., monoclinic 2/*m* (non-polar) → Removal of *I* → monoclinic 2 (polar)

An example of multi-spin variables which induces ME coupling
- Vector spin chirality -

- **Ferroelectricity driven by spiral spin order**

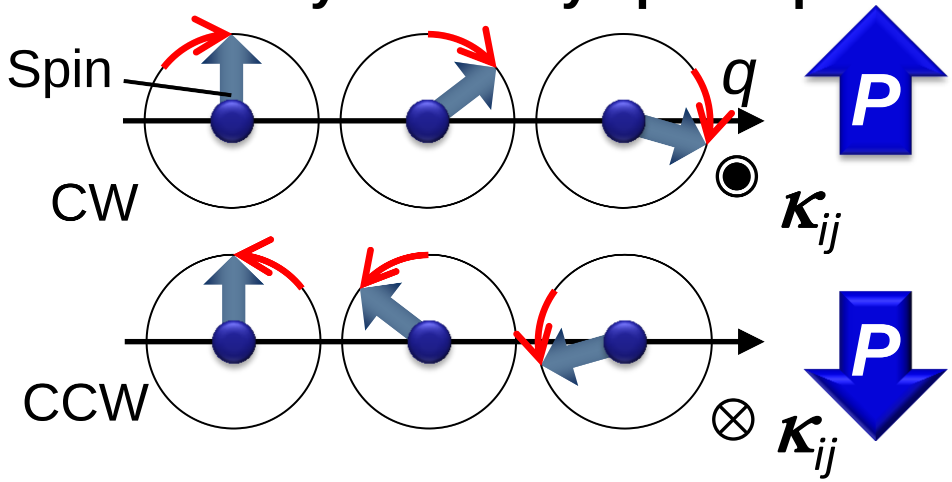

Y. Yamasaki et al.,
PRL 98, 147204 (2007).

Vector spin chirality

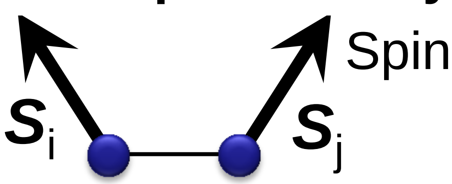

$$\boldsymbol{\kappa}_{ij} \equiv \boldsymbol{S}_i \times \boldsymbol{S}_j$$

Spin-current (or Inverse DM) interaction

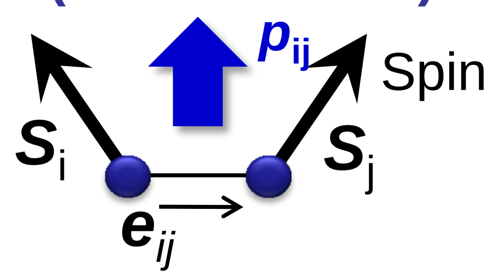

$$\boldsymbol{p}_{ij} \propto \boldsymbol{e}_{ij} \times (\boldsymbol{S}_i \times \boldsymbol{S}_j)$$

Katsura et al., PRL (2005); Sergienko & Dagotto PRB (2006)

✓ **Polarization *P* ⟺ Chirality κ_{ij}**

Vector spin chirality can be detected as electric polarization *P* through ME coupling.

Outline

1. Introduction: Magnetoelectric effect & multi-spin variables

2. Room-temperature magnetoelectrics possibly by spin spiral

Hexaferrites $Sr_3Co_2Fe_{24}O_{41}$ with the Z-type structure

3. Observation of Spin-chiral Domains in Multiferroic Hexaferrites by Scanning Resonant X-ray

Hexaferrites $Ba_{0.5}Sr_{1.5}Zn_2Fe_{12}O_{22}$ with the Y-type structure

4. Magnetoelectric effect observed in a magnetically-disordered system

XY-like spin-glass $(Ni,Mn)TiO_3$ with the ilmenite structure

List of spin-spiral-driven ferroelectrics

Compound	Crystal structure	Magnetic ion	Proposed spin structure	Temperature range (K)	Ref.
$RMnO_3$ (R=Tb, etc.)	O (mmm) [perovskite]	Mn^{3+} S=2	cycloidal	≤ 28	Kimura *et al.* (2003)
$Ni_3V_2O_8$	O (mmm)	Ni^{2+} S=1	cycloidal	3.9~6.3	Lawes *et al.* (2005)
$(Ba,Sr)_2M_2Fe_{12}O_{22}$	R (-3m) [haxaferrite]	Fe^{3+} S=5/2	screw, L-conical (B=0) T-conical (B>0)	≤ ~110	Kimura *et al.* (2005)
$CuFeO_2$	R -3m [delafossite]	Fe^{3+} S=5/2	collinear(B=0) screw (B>0)	≤ 11	Kimura *et al.* (2005)
$CoCr_2O_4$	C (m3m) [spinel]	Co^{2+} Cr^{3+} S=3/2 S=3/2	T-conical	≤ 26	Yamasaki *et al.* (2006)
$MnWO_4$	M (2/m) [walframite]	Mn^{2+} S=5/2	cycloidal	7~12.5	Taniguchi *et al.* (2006)
$RbFe(MoO_4)_2$	R (-3m)	Fe^{3+} S=5/2	screw	≤ 3.8	Kenzelmann *et al.* (2006)
$LiCu_2O_2$	O (mmm)	Cu^{2+} S=1/2	cycloidal	≤ 23	Park *et al.* (2007)
$LiCuVO_4$	O (mmm)	Cu^{2+} S=1/2	cycloidal	≤ 2.4	Naito *et al.* (2007)
CuO	M (2/m) [tenorite]	Cu^{2+} S=1/2	cycloidal + screw	212~230	Kimura *et al.* (2008)
$ACrO_2$ (A=Ag, Cu)	R (-3m) [delafossite]	Cr^{3+} S=3/2	screw	≤ 24	Seki *et al.* (2008)
$FeVO_4$	Tri (-1)	Fe^{3+} S=5/2	cycloidal	≤ 16	Daoud-Aladine *et al.* (2009)
$CuCl_2$	M (2/m) [distorted CdI_2]	Mn^{2+} S=5/2	cycloidal	≤ 24	Seki *et al.* (2010)

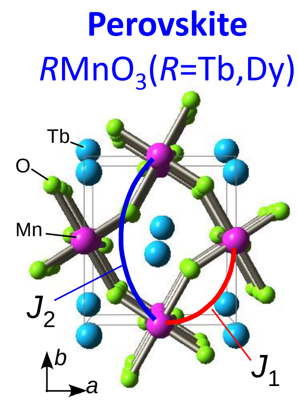

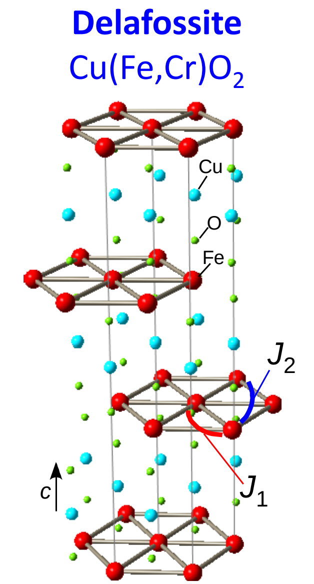

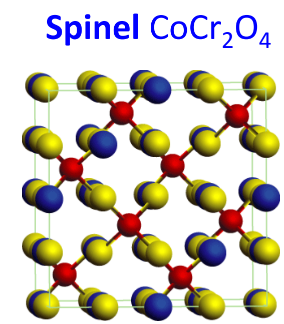

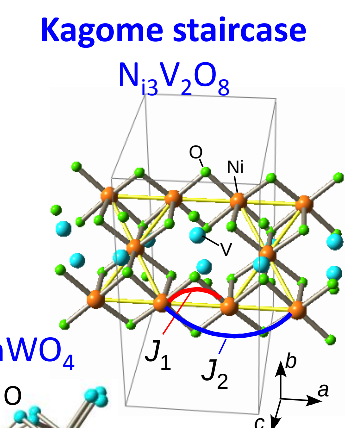

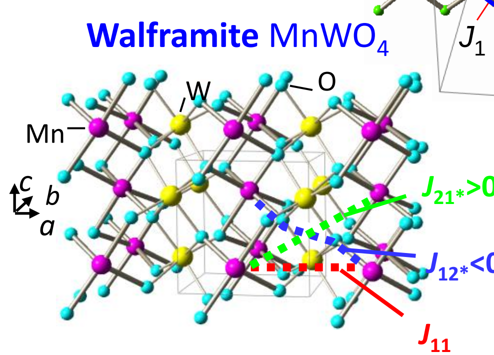

High-*T* multiferriocs - Y-type hexaferrite $(Ba,Sr)_2(Zn,Mg)_2Fe_{12}O_{22}$ -

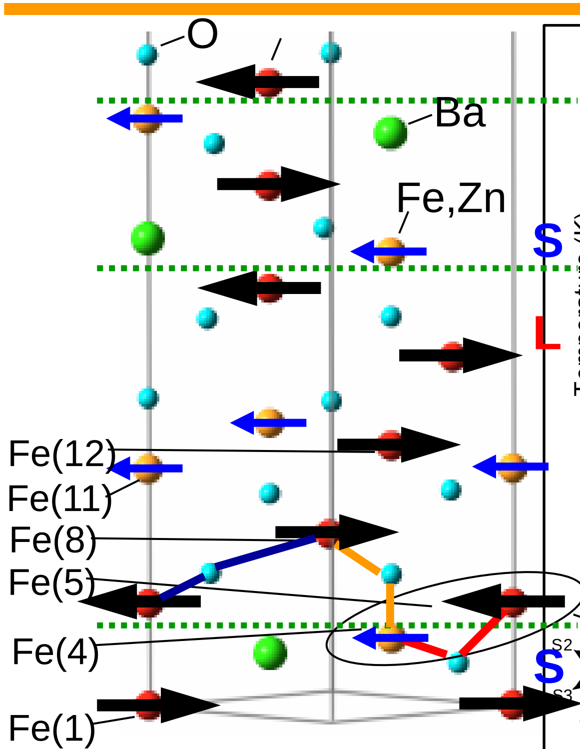

Kimura et al., PRL. 94, 137201 (2005)

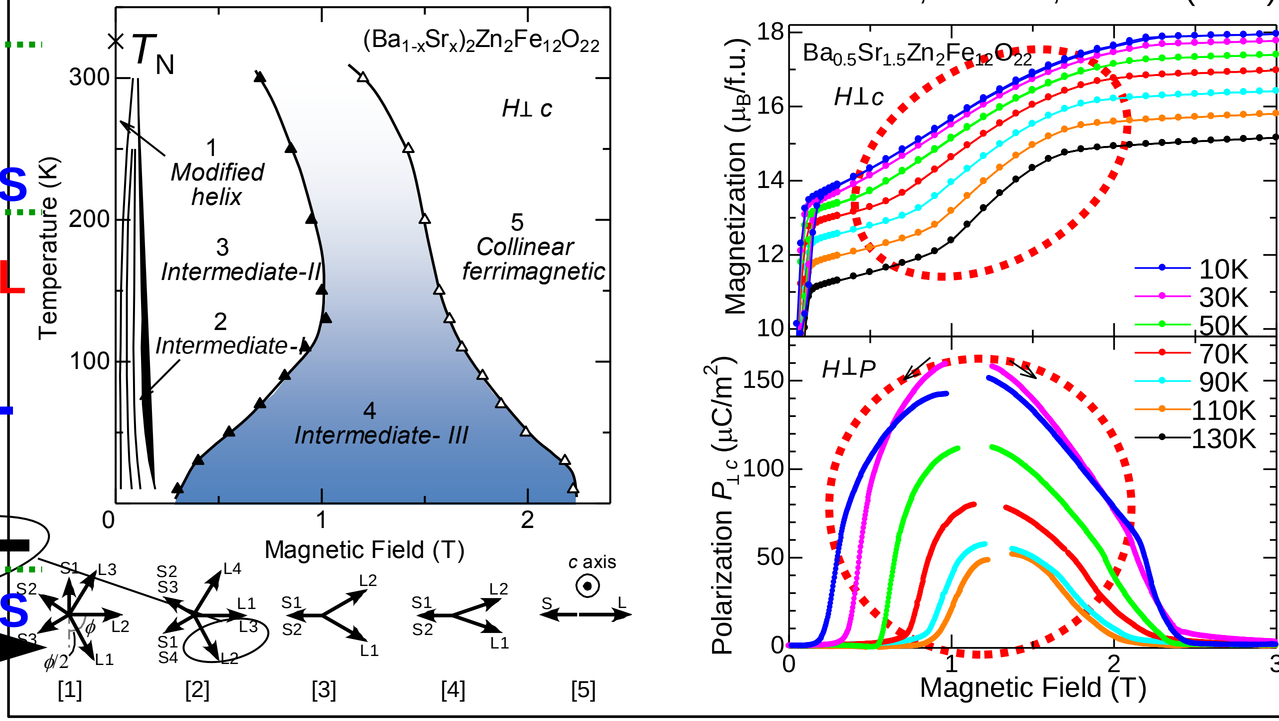

Ferroelectric intermediate-III phase survives up to near room temperature.

However, suppression of resistivity does not allow experimental observation of polarization above ~110K.

ME effect
at low *H* (~mT)
but only at low *T*
(<~30K)

Ishiwata et al. Science 319, 1643 (2008).

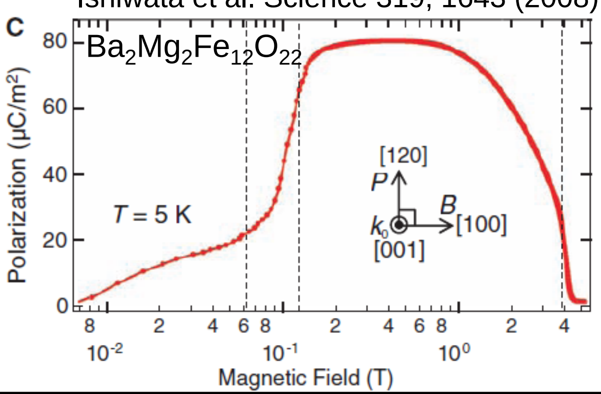

Chun et al. PRL 104, 037204 (2010).

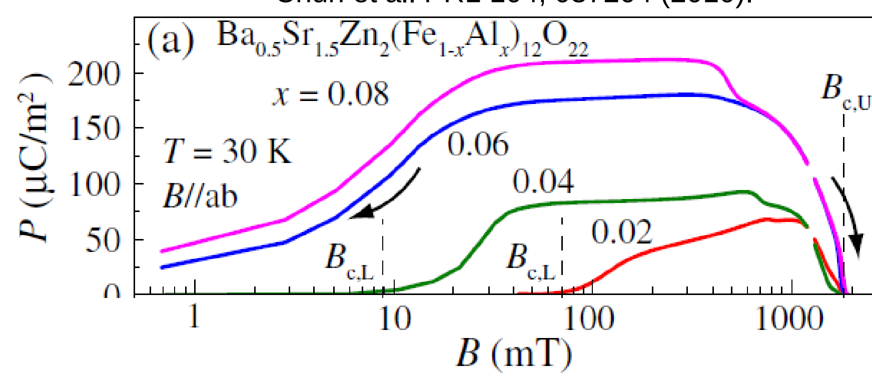

Classification of hexagonal ferrites

- Stacking sequence composed of 3 types of blocks-

J. Smit & H.P.J. Wijn, Ferrite (Philips' Technical Library, 1959)

R

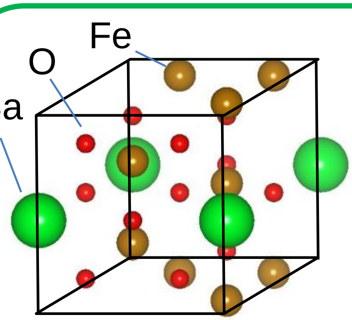

R-block

$[BaFe_6O_{11}]^{2-}$

S

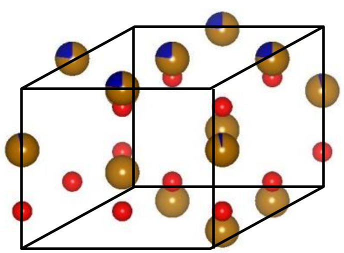

S-block (Spinel)

$M_2^{2+}Fe_4O_8$

T

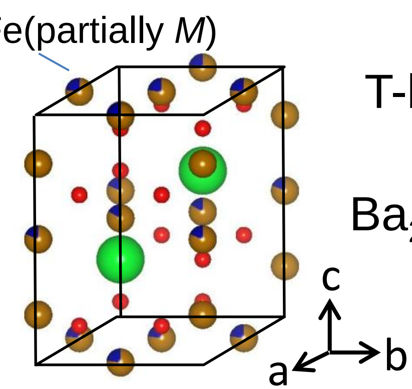

T-block

$Ba_2Fe_8O_{14}$

	Chem. form.	stacking	c(Å)	S.G.
M	$BaFe_{12}O_{19}$	RSR^*S^*	23.19	$P6_3/mmc$
W	$BaM_2Fe_{16}O_{27}$	$RS_2R^*S^*_2$	32.84	$P6_3/mmc$
Y	$Ba_2M_2Fe_{12}O_{22}$	$(TS)_3$	43.56	$R\text{-}3/m$
Z	$Ba_3M_2Fe_{24}O_{41}$	$RSTSR^*S^*T^*S^*$	52.3	$P6_3/mmc$
X	$Ba_2M_2Fe_{28}O_{46}$	$(RSR^*S^*)_3$	84.11	$R\text{-}3/m$
U	$Ba_4M_2Fe_{36}O_{60}$	$(RSR^*S^*TS^*)_3$	113	$R\text{-}3/m$

M-type

(magnetoplumbite)

$BaFe_{12}O_{19}$

(c=23.19 Å)

Refrigerator magnet

Crystal structures of 6 main types of hexaferrites

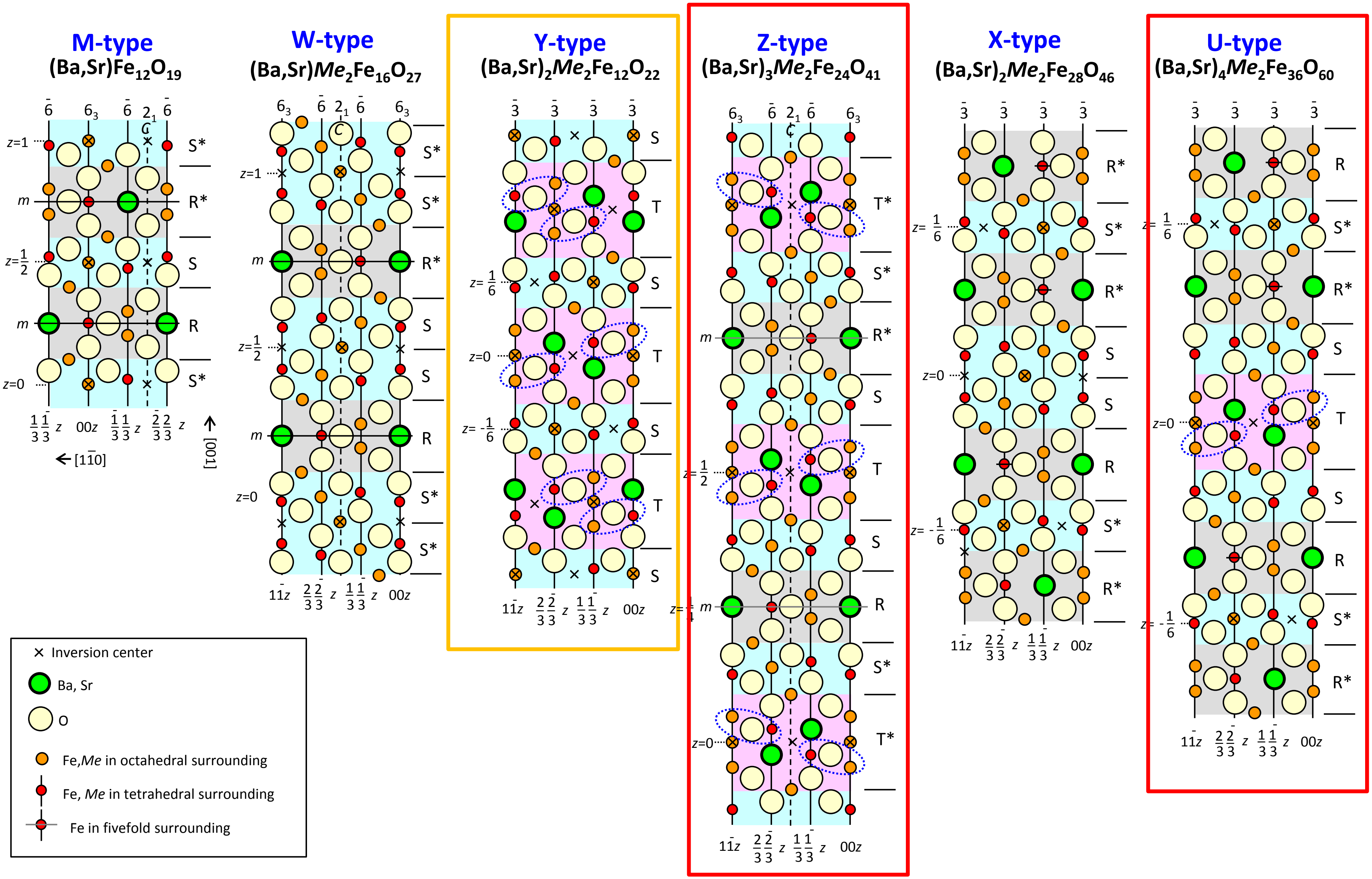

Former studies on magnetism of Z-type hexaferrites

Noncollinear Magnetic Structures in Hexagonal Ferrites of the $Ba_{3-x}Sr_{3-x}Zn_2Fe_{24}O_{41}$ *(Z) System*

M. I. NAMTALISHVILI, O. P. ALESHKO-OZHEVSKIĬ, AND I. I. YAMZIN

Crystallography Institute, USSR Academy of Sciences

Submitted July 26, 1971

Zh. Eksp. Teor. Fiz. **62**, 701–709 (February, 1972)

Single crystals are investigated at temperatures from 78°K up to the Curie point for values x=2.4; 2.0; 1.5; 0. The neutron diffraction pattern is explained on the basis of angular magnetic structures which combine spin collinearity within certain blocks of the unit cell and noncollinearity of their summary magnetic moments. Noncollinearity is observed in crystals in which a significant part of the ions are replaced by strontium. With increase of strontium concentration and lowering of temperature, a deviation of the spins from the hexagonal axis occurs and the angle between directions of the summary magnetic moments of the blocks increases. Moreover, spin modulation at temperatures below 110–120°K arises. The noncollinearity is ascribed to violation in the exchange interaction scheme on localization of zinc ions in crystallographic positions at the block boundaries.

$(Ba,S)_3Zn_2Fe_{24}O_{41}$

Zh.Eksp. Teor. Fiz. 62, 701 (1972)

Noncollinear spin structure?

Pullar et al., Mater. Res. Bull. 36, 1531 (2001).

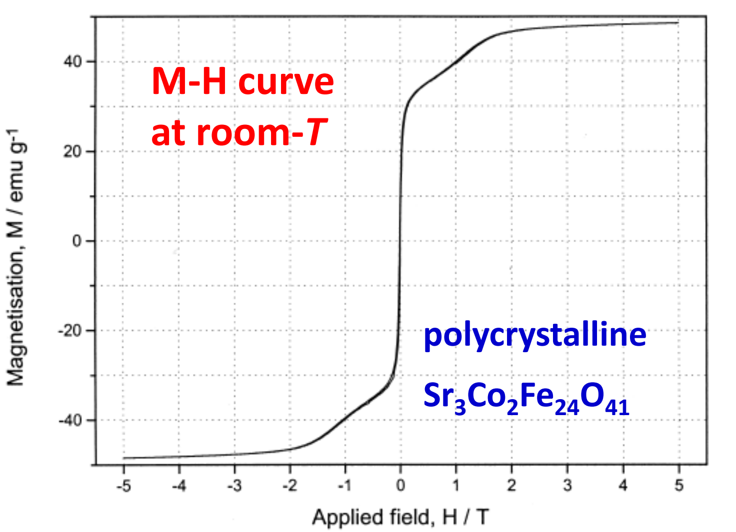

Takada et al., JAP 100, 043904 (2006).

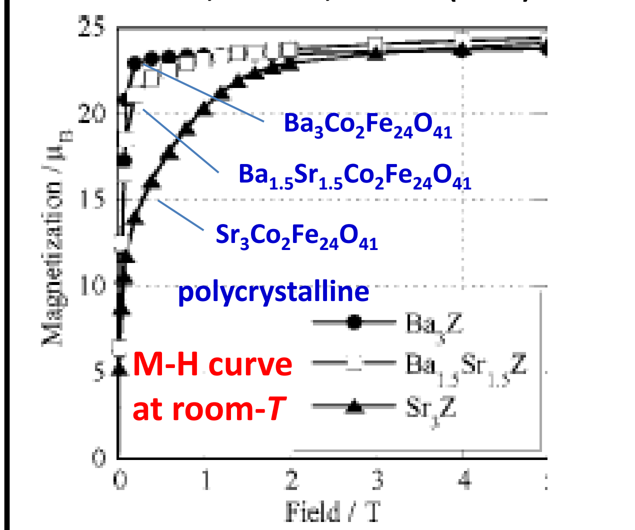

M of $Sr_3Co_2Fe_{24}O_{41}$ increases in a stepwise fashion.

→ Similar to magnetoelectric Y-type hexaferrites

Magnetic & magnetoelectric properties of Z-type $Sr_3Co_2Fe_{24}O_{41}$

polycrystalline ceramics sintered in oxygen.

Kitagawa et al., Nature Mater. 9, 797 (2010).

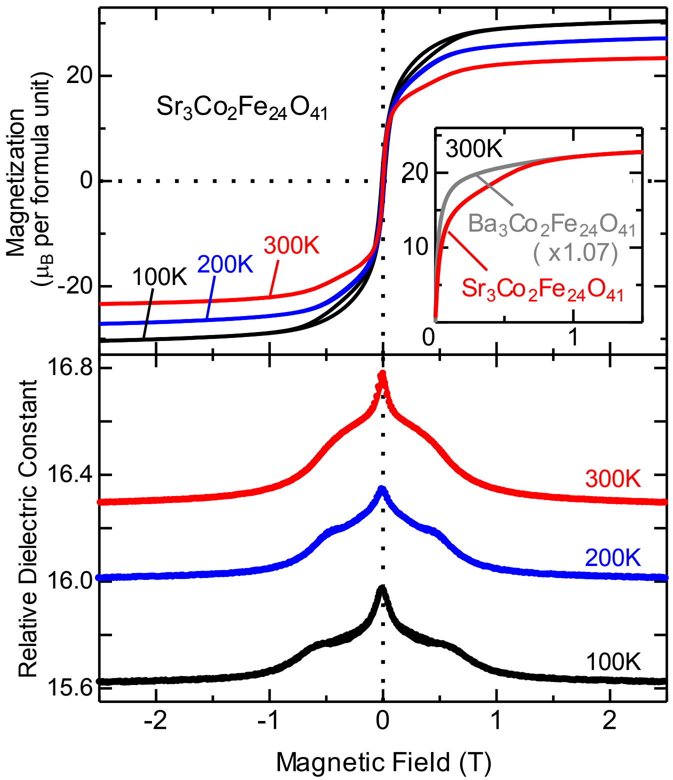

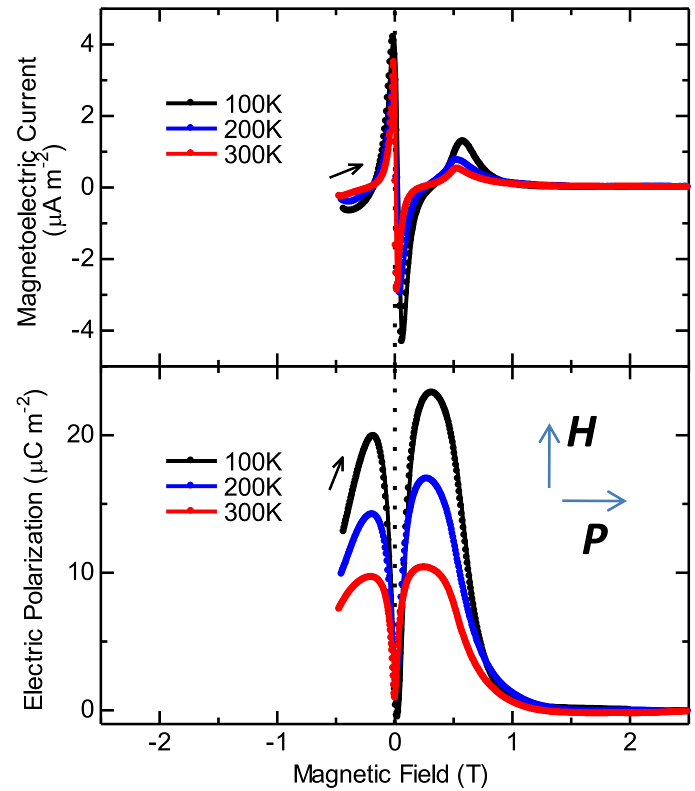

ME_H effects are observed at a wide *T* range including room temperature.

*ME coefficient defined as $\alpha=\mu_0 dP/dB$

The α exceeds 1×10^{-10} s/m below 0.04T and reached a maximum ~2.5×10^{-10}s/m at 0.003T.

(c.f. α in Cr_2O_3: 4×10^{-12} s/m; α in Z-type single crystal: 3×10^{-9} s/m by Chun et al. PRL 108, 177201 (2012)

Recently, ME_E effects are also observed at room temperature.⇒

Electric control of Magnetism in Z-type hexaferrites

Change in Magnetization by *E*

Chun et al. Phys. Rev. Lett. 108, 177201 (2012)

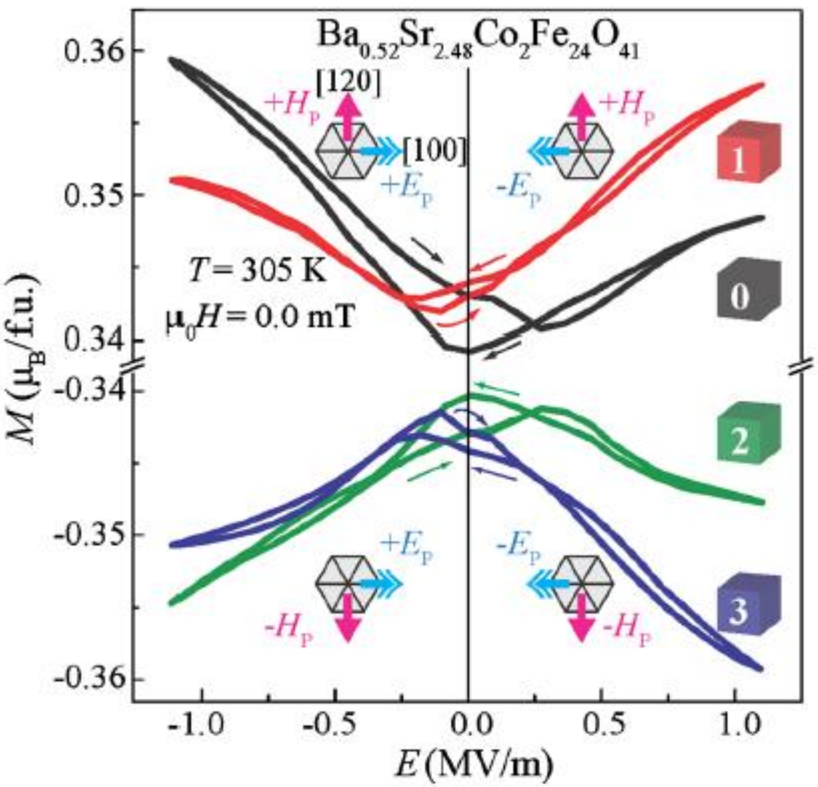

Change in magnetic permeability at GHz range by *E*

Ebnabbasi et al. Phys. Rev. B 86, 024430 (2012)

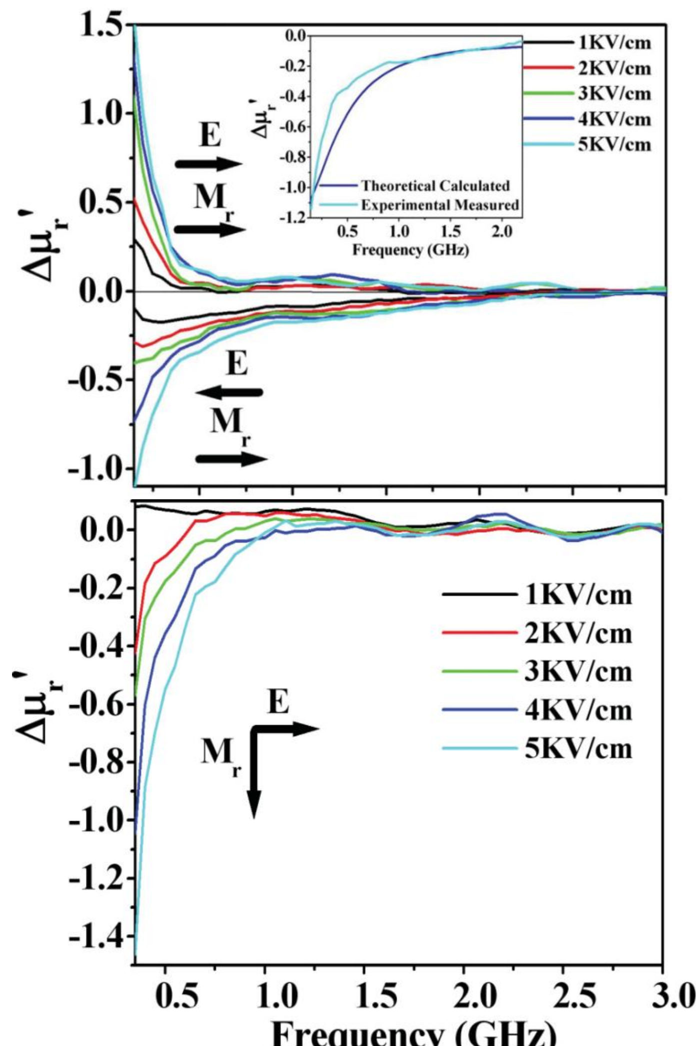

Understanding of the origin of the ME effect of Z-type $Sr_3Co_2Fe_{24}O_{41}$

Neutron powder diffraction (at JRR-3 of JAEA, Tokai, Japan) **Soda et al., PRL 106, 087201 (2011).**

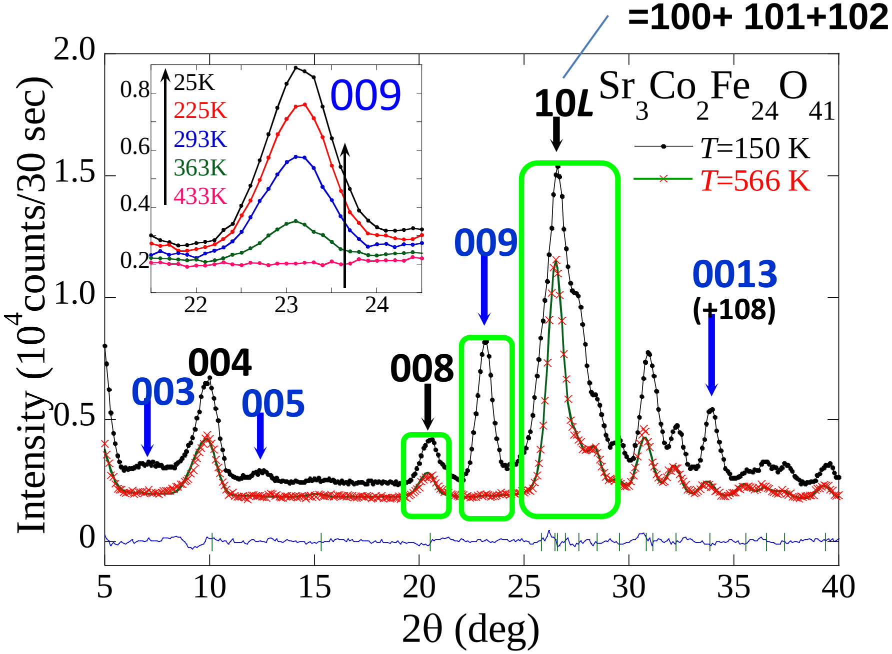

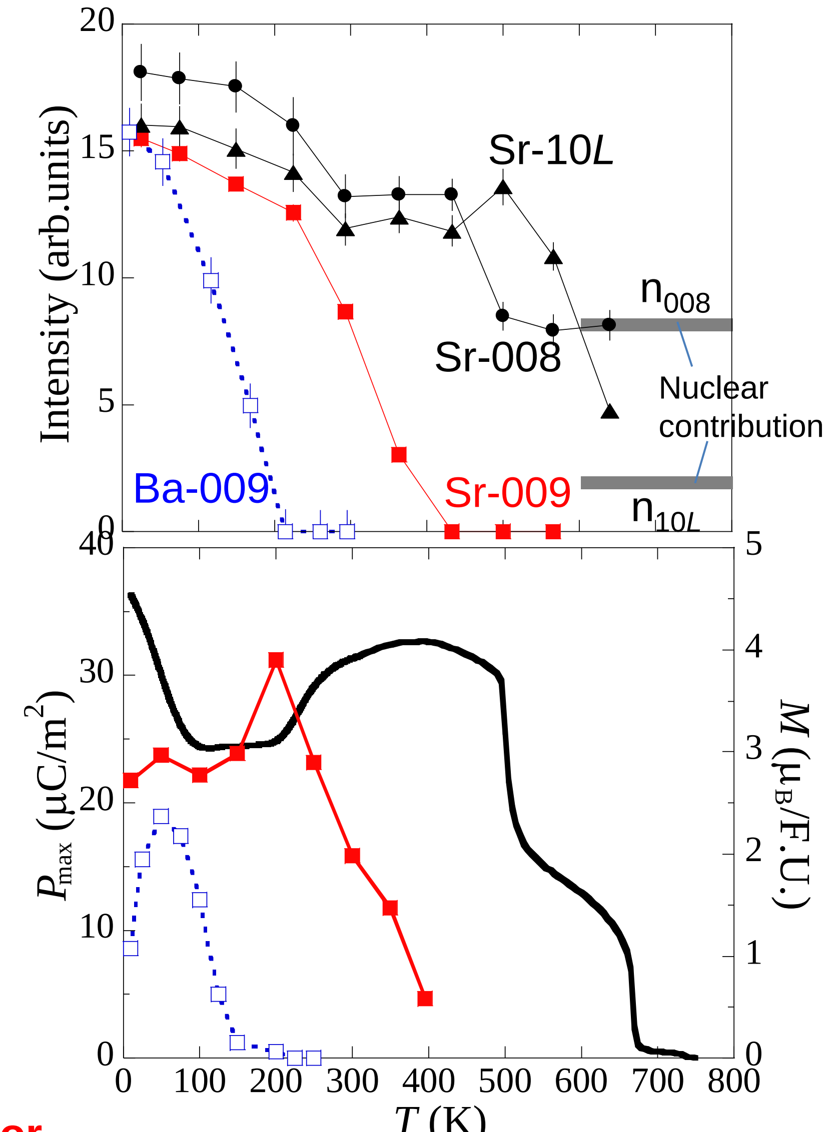

***Below ~670K**, a ferrimagnetic ordering where t ... s.

***Below ~500K**, the moments rotate toward the a

***Below ~400K**, a new magnetic order **[(0,0,l_o)]** b .

The magnetic order with (0,0,1) propagation vector has intimate connection with the room-temperature ME effect in $Sr_3Co_2Fe_{24}O_{41}$.

Origin of magnetoelectric effect –Neutron diffraction, *H*-dependence-

Soda et al., PRL 106, 087201 (2011).

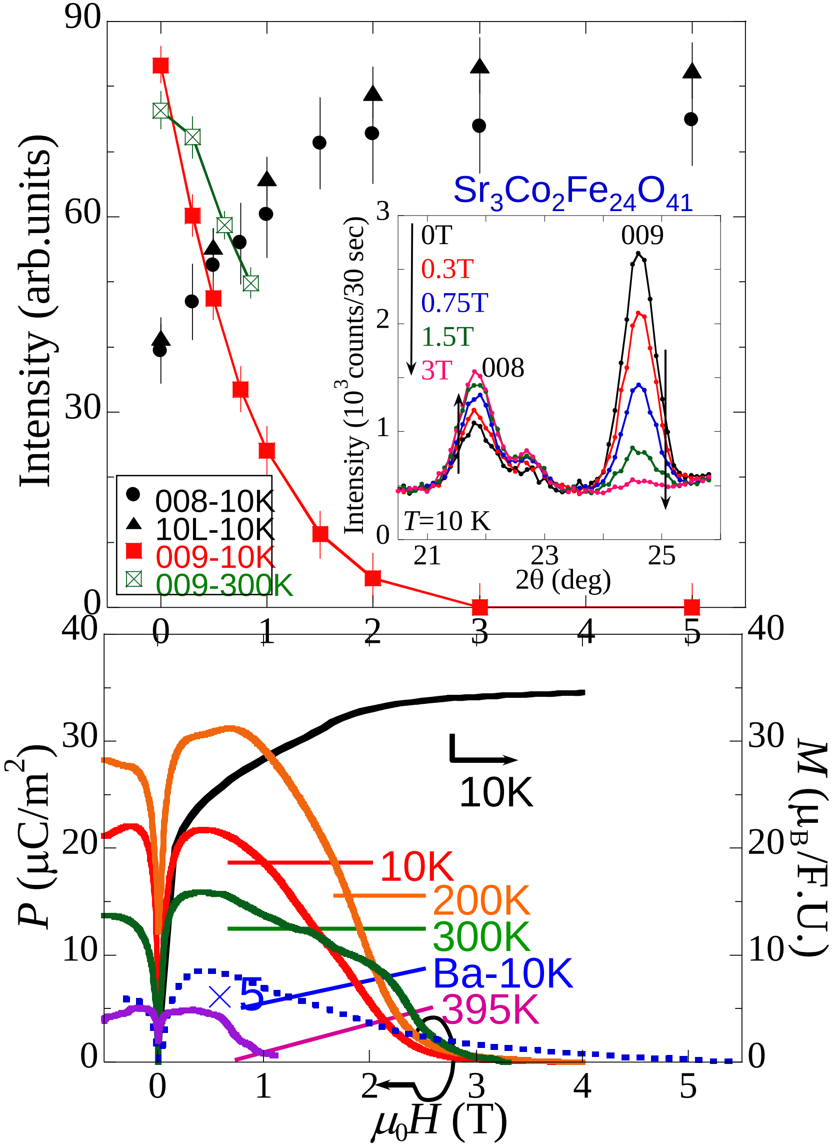

Proposed spin structure related to ME effect in Z-type Sr$_3$Co$_2$Fe$_{24}$O$_{41}$

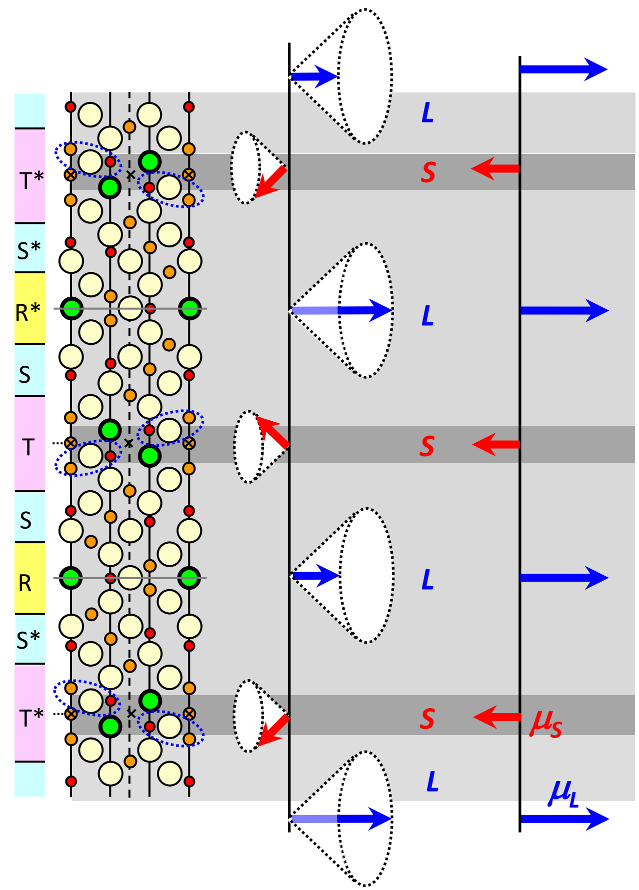

In analogy with Y-type hexaferrites, the r.t. ME effect can be understood in terms of *P* induced by a transverse conical spin structure through the inverse DM mechanism.

Domain structures in ferroic solids

Formation of domain structures by phase transitions in solids

ferromagnet

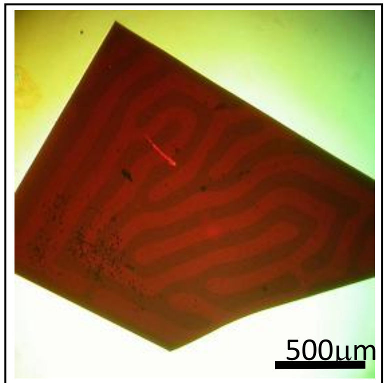

Magnetic domains

ferroelectrics

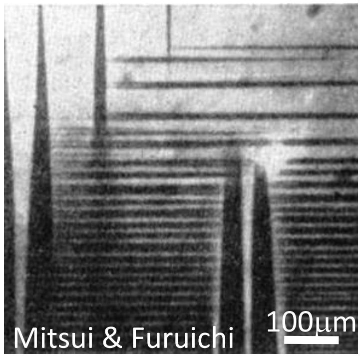

Ferroelectric domains

ferroelastics

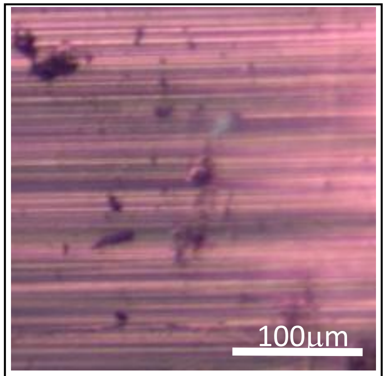

Twins

Left-handed spin-helicity (0) Right-handed spin-helicity (1)

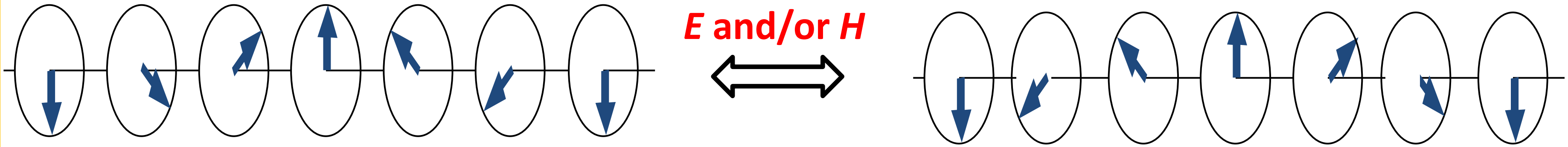

**Observation of spiral-spin domains in spiral magnets by scanning resonant x-ray microdiffraction*

Outline

1. Introduction: Magnetoelectric effect & multi-spin variables

2. Room-temperature magnetoelectrics possibly by spin spiral

Hexaferrites $Sr_3Co_2Fe_{24}O_{41}$ with the Z-type structure

3. Observation of Spin-chiral Domains in Multiferroic Hexaferrites by Scanning Resonant X-ray

Hexaferrites $Ba_{0.5}Sr_{1.5}Zn_2Fe_{12}O_{22}$ with the Y-type structure

4. Magnetoelectric effect observed in a magnetically-disordered system

XY-like spin-glass $(Ni,Mn)TiO_3$ with the ilmenite structure

Imaging spiral magnetic domains in Ho by circularly polarized Bragg diffraction

J.C. Lang et al., J. Appl. Phys. 95, 6537 (2004).

Ho metal

[spiral magnetic order with (0,0, $L \pm \tau$) below T_N=133K]

X-ray energy E~ 8.071 eV (~ Ho L_3-edge 2p → 5d)

Size of circularly polarized x-ray beam

25 μm × 25μm

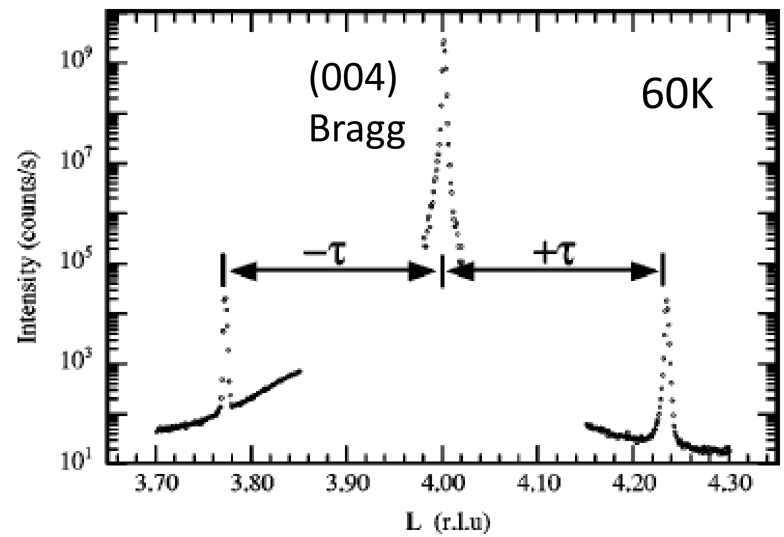

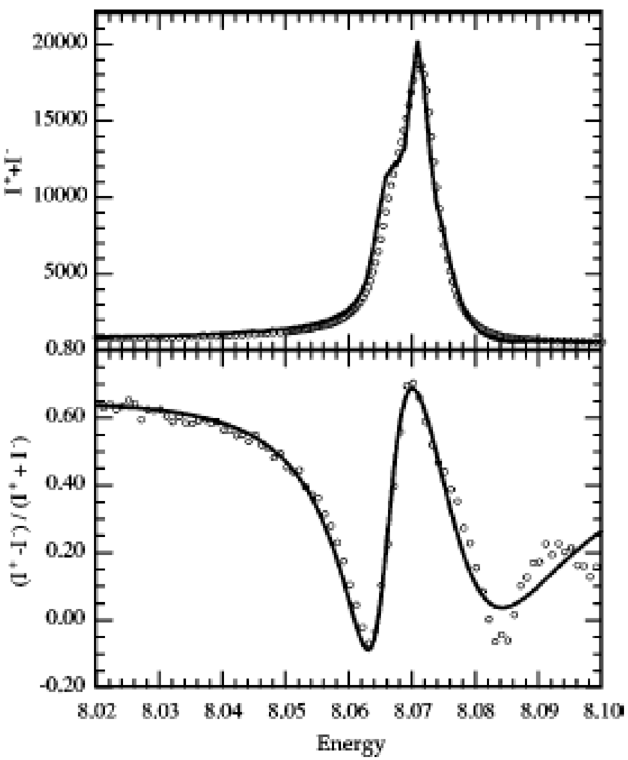

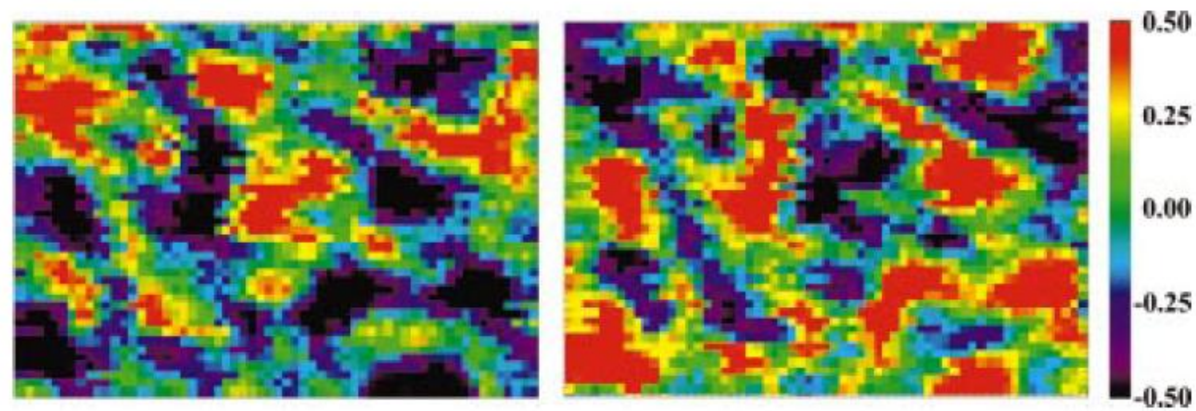

(0.6X0.45mm^2)

Imaging spiral magnetic domains in multiferroics by circularly polarized X-ray

$Ni_3V_2O_8$

Fabrizi, Phys. Rev. B **82**, 024434 (2010).

Nonresonant X-ray

Beam size ≈ 380 × 250 μm^2

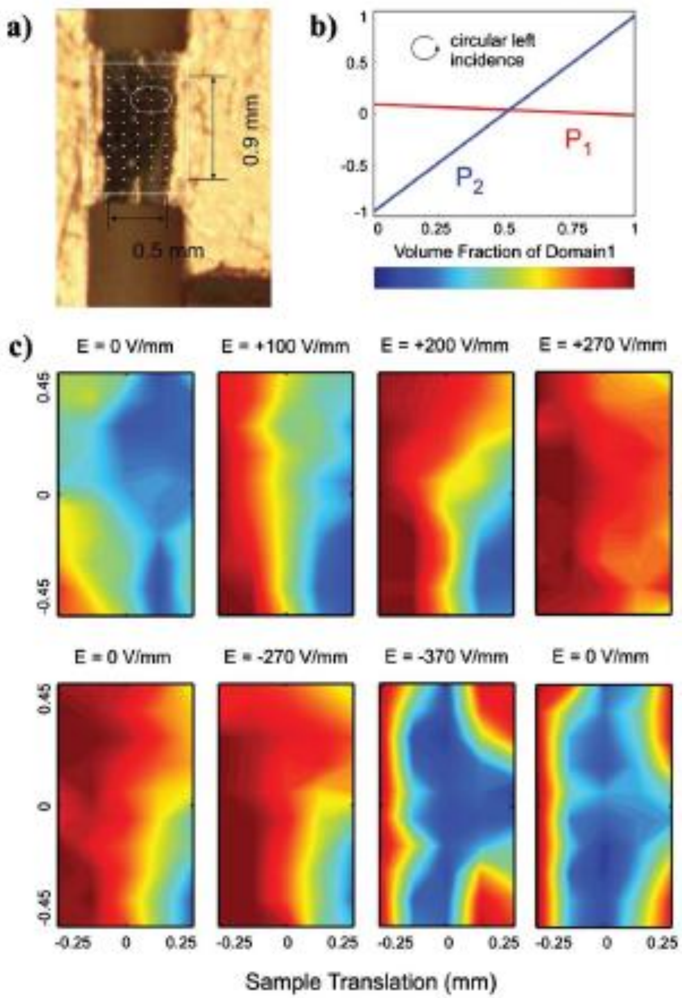

$DyMnO_3$

Schierle, Phys. Rev. Lett. **105**, 167207 (2010).

X-ray energy : Dy M_5-edge

Beam size ≈ 300 × 100 μm^2

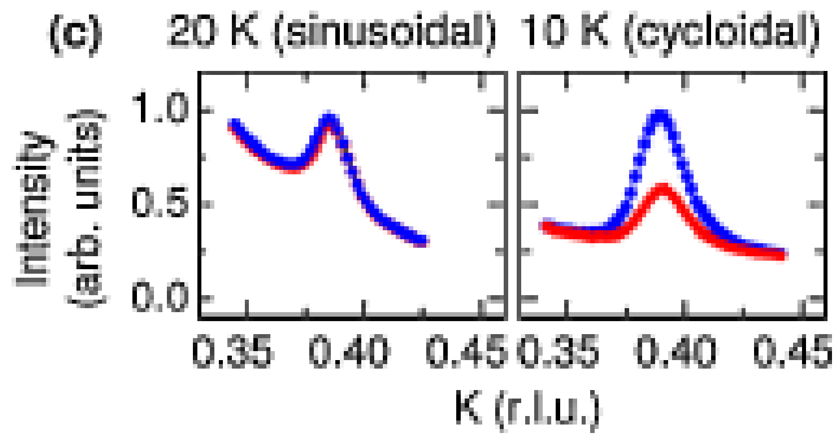

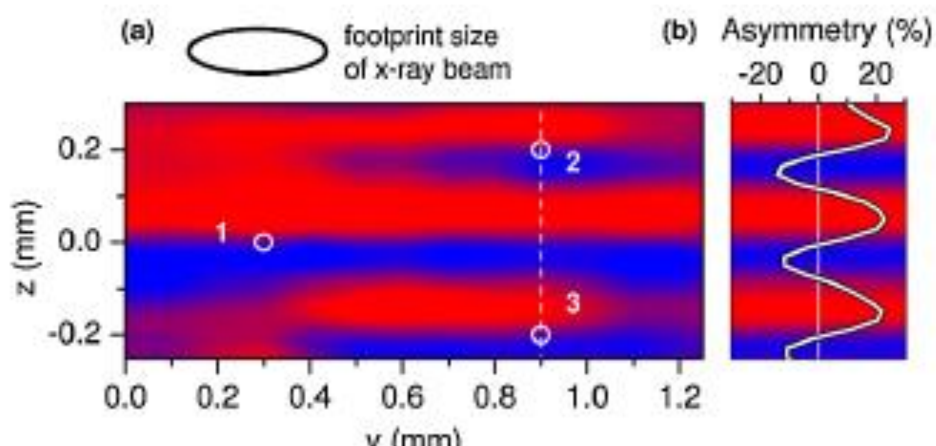

Imaging spin-chiral domains in Y-type $Ba_{0.5}Sr_{1.5}Zn_2Fe_{12}O_{22}$ by circularly polarized X-ray

Sample **Y-type $Ba_{0.5}Sr_{1.5}Zn_2Fe_{12}O_{22}$ T_N ~ 310 K magnetic satellite $(0,0,3n\pm\varepsilon)$, c –axis length ~43 Å)**

Experimental conditions (@BL17SU, Spring-8)

Incident x-ray energy 710 eV (λ ~ 17 Å)
[at Fe L_3 edge ($2p \rightarrow 3d$)]

Beam size ~30 x 15 μm²
with a 25 μm step

Penetration depth ~40 nm

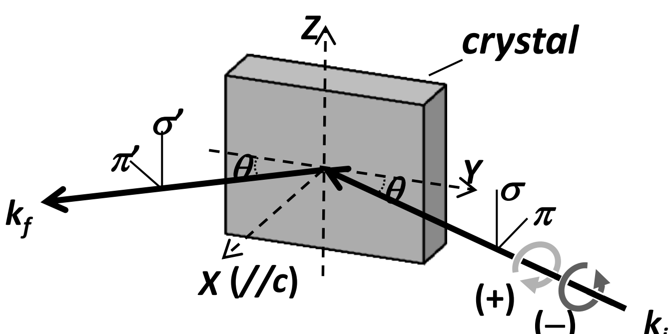

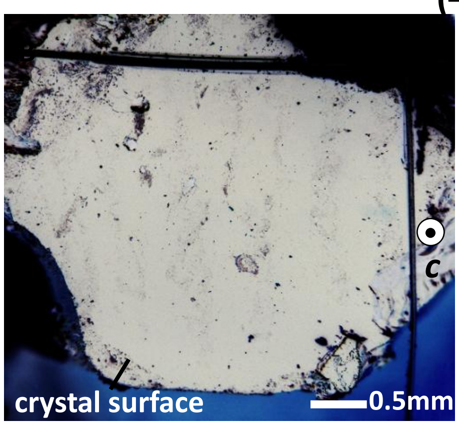

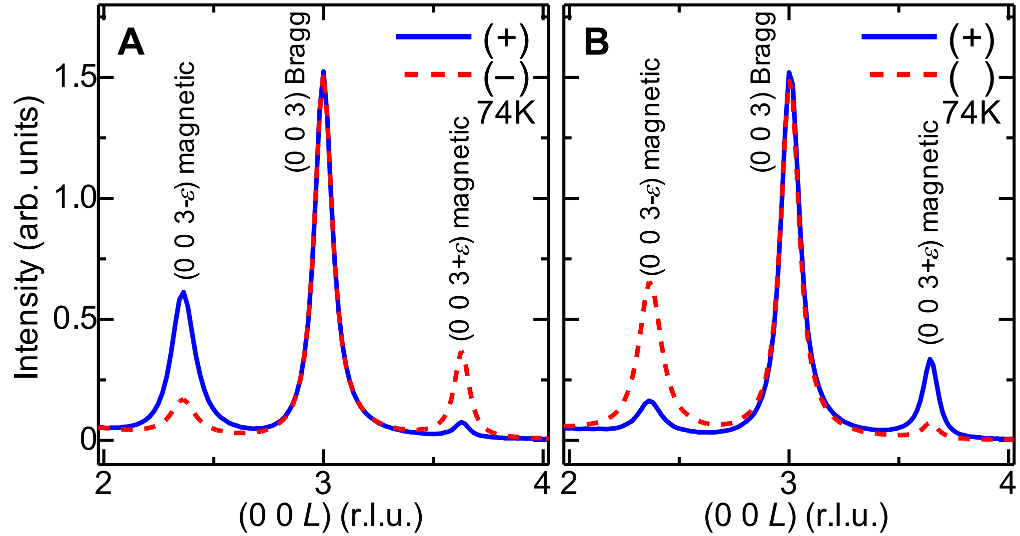

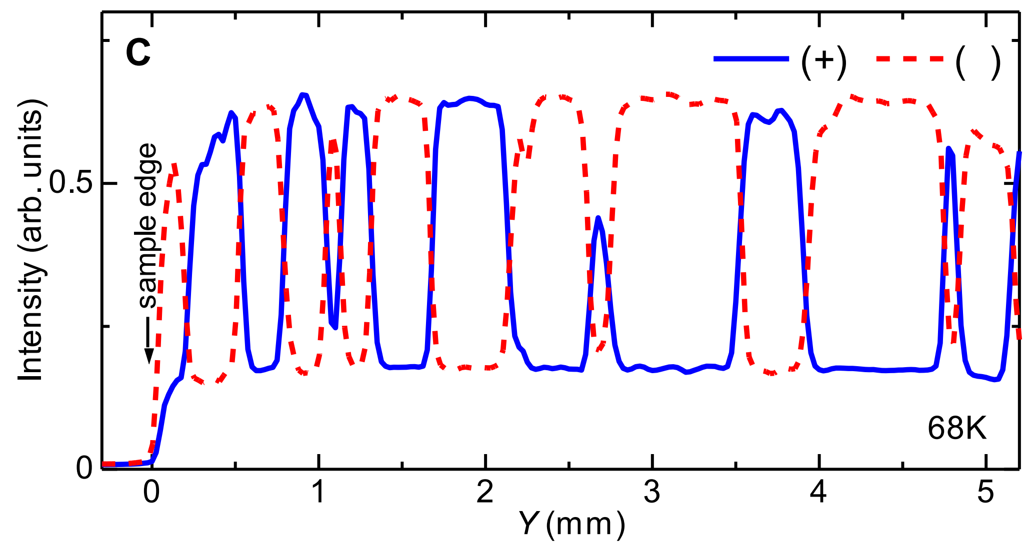

Spatial images of spin-chiral domain structure in $Ba_{0.5}Sr_{1.5}Zn_2Fe_{12}O_{22}$ at 68 K

Y. Hiraoka et al., PRB 84, 064418 (2011).

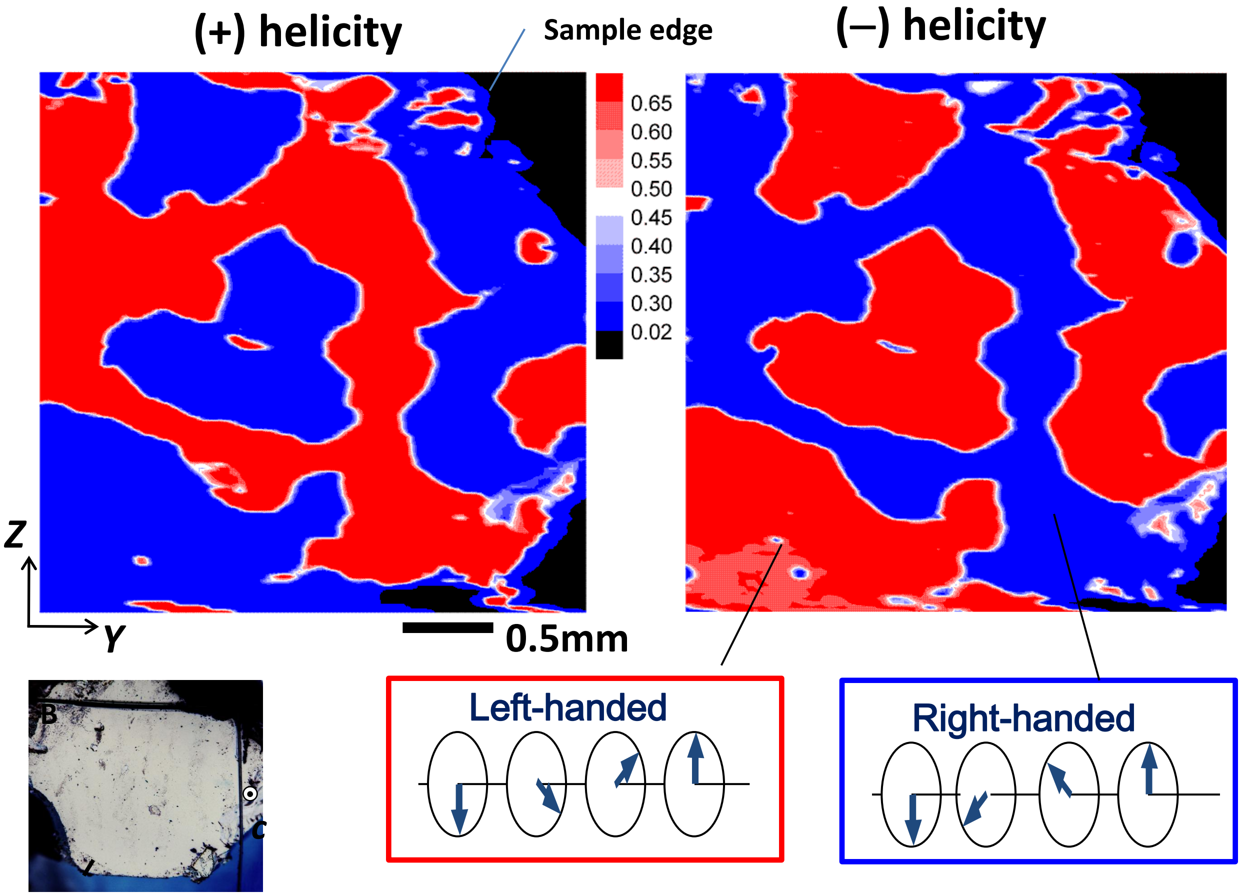

c.f. Data of a crystal with a rough surface

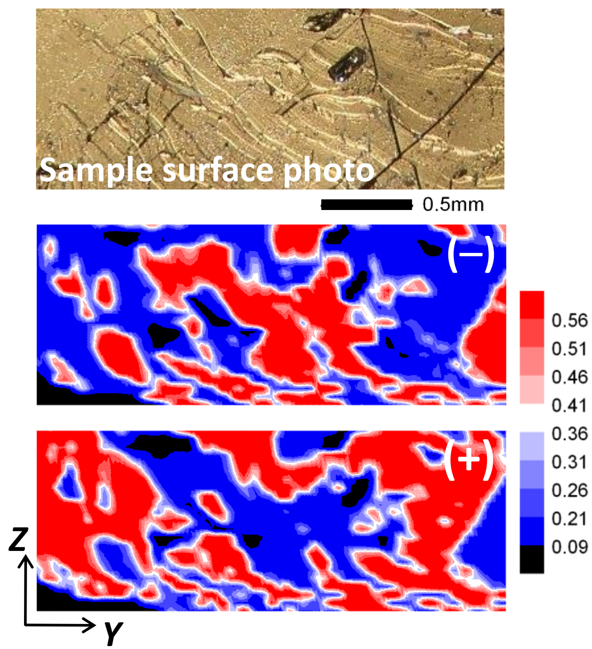

*Red and blue regions correspond to either a left- or right-handed spin-chiral monodomain.
*The observed domains are irregular in shape with a size on a submilimeter scale.

*There is a tendency that the domain boundaries are clamped at surface defects.
*The observed domains were apparently smaller in size than those on a smooth surface.

Outline

1. Introduction: Magnetoelectric effect & multi-spin variables

2. Room-temperature magnetoelectrics possibly by spin spiral

Hexaferrites $Sr_3Co_2Fe_{24}O_{41}$ with the Z-type structure

3. Observation of Spin-chiral Domains in Multiferroic Hexaferrites by Scanning Resonant X-ray

Hexaferrites $Ba_{0.5}Sr_{1.5}Zn_2Fe_{12}O_{22}$ with the Y-type structure

4. Magnetoelectric effect observed in a magnetically-disordered system

XY-like spin-glass $(Ni,Mn)TiO_3$ with the ilmenite structure

Theoretically, multi-spin variables can be nonzero even in the absence of long-range magnetic order.

Chiral spin liquid phase in helimagnets

F. Cinti et al., PRL 100, 057203 (2008); PRB 83, 174414 (2011).

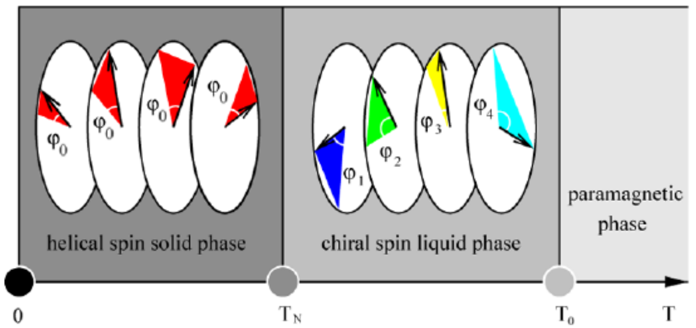

FIG. 1 (color online). Schematic representation of Villain's conjecture. In the chiral spin liquid phase, corkscrews all turning clockwise (or all anticlockwise) with in general $\varphi_i \neq \varphi_j$. In the helical spin solid phase, same angle value φ_0 for all spins.

Spin-chirality decoupling in spin-glass system

H. Kawamura, PRL 68, 3785 (2011);
J. Phys. Condens. Matter 23, 164210 (2011).

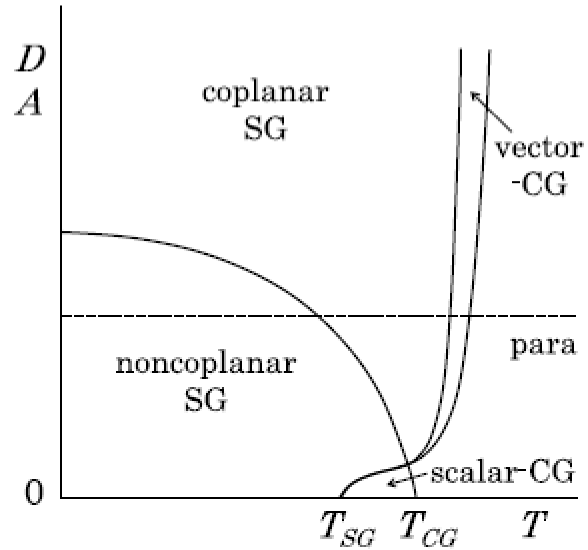

Figure 1. Phase diagram of the XY-like SG with an easy-plane-type uniaxial magnetic anisotropy in the uniaxial anisotropy versus the temperature plane. T_{CG} and T_{SG} represent the chiral-glass and the spin-glass transition temperatures of the fully isotropic Heisenberg system.

⇨ **It is possible that ME materials are found in magnetically-disordered phases.**

Spin chirality in spin glass system

A chirality driven mechanism for spin-glass transitions

H. Kawamura, PRL 68, (1992) 3785.

Heisenberg spin glass

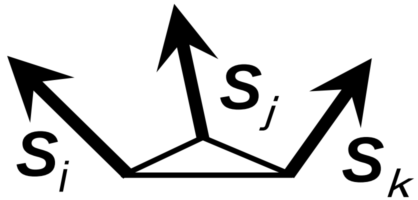

$S_i \cdot (S_j \times S_k)$

Anomalous Hall effect due to scalar spin chirality

T. Taniguchi, et al., PRL 93, (2004) 246605.

XY spin glass

Vector spin chirality can exist.

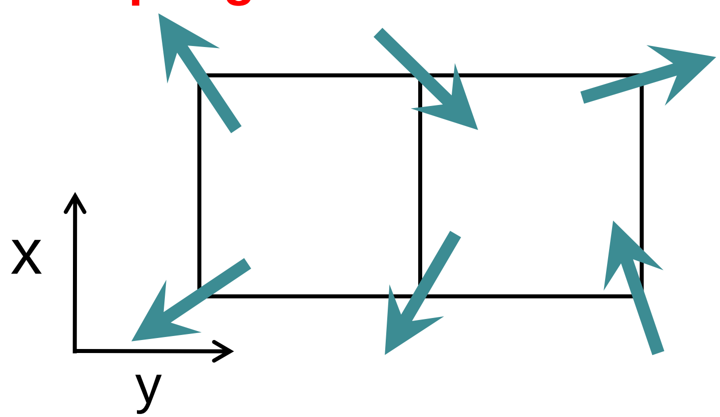

H. Kawamura, J. Phys. Cond. Matter 23, 164210 (2011).

Can we detect vector spin chirality in spin glass system though magnetoelectric coupling?

Example compounds showing insulating & XY-like spin glass state

$^*Rb_2Mn_{1-x}Cr_xCl_4$	K. Katsumata et al., PRB 25, 428 (1982).
$^*Ni_xMn_{1-x}TiO_3$	A. Ito et al., JMMM 104, 1637 (1992).

Crystal structure of $Ni_xMn_{1-x}TiO_3$

ilmenite structure

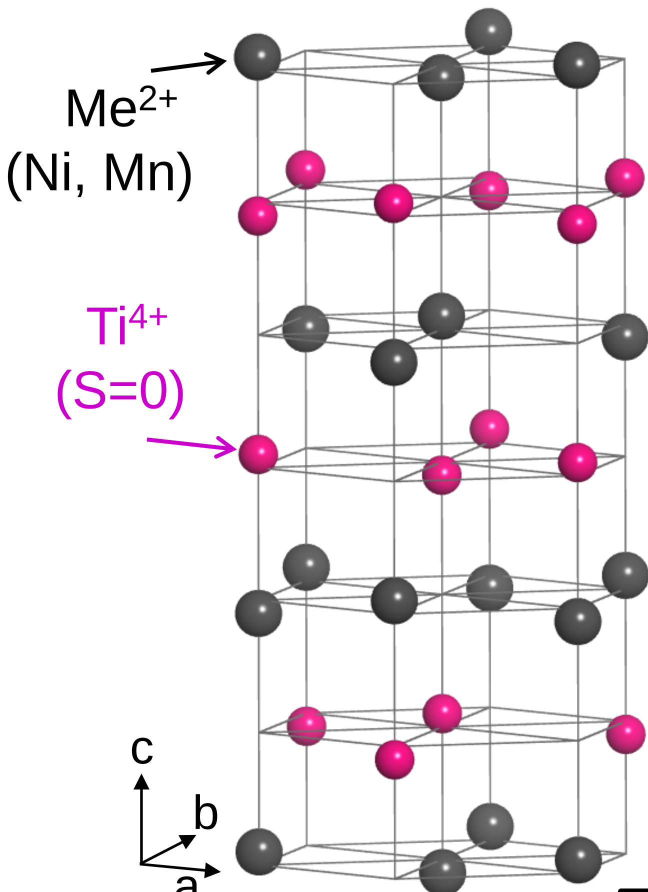

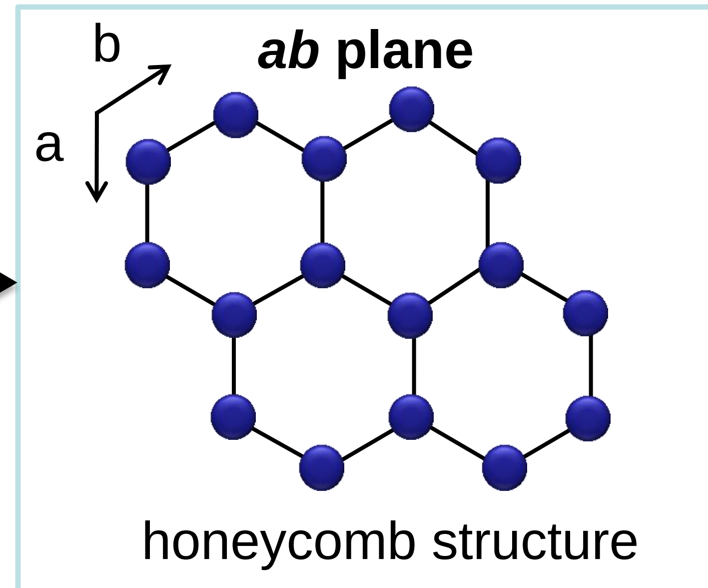

- **Alternating stack of Me^{2+} & Ti^{4+}**
- **Only Me (Ni, Ni) ions are magnetic.**
- **Space group $R\bar{3}$ $\longrightarrow$ centrosymmetric**

Magnetic phase diagram of $Ni_xMn_{1-x}TiO_3$

$MnTiO_3$

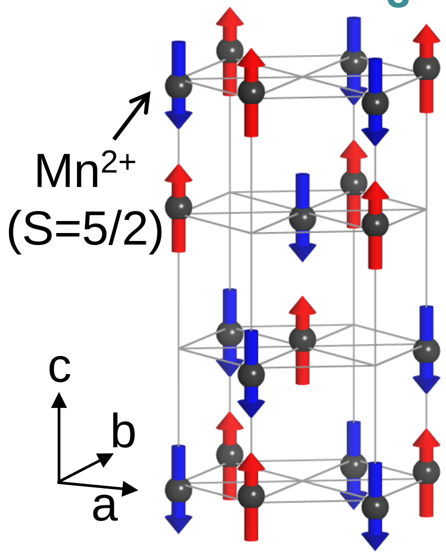

A. Ito *et al.*, JMMM104-107, 1637 (1992).

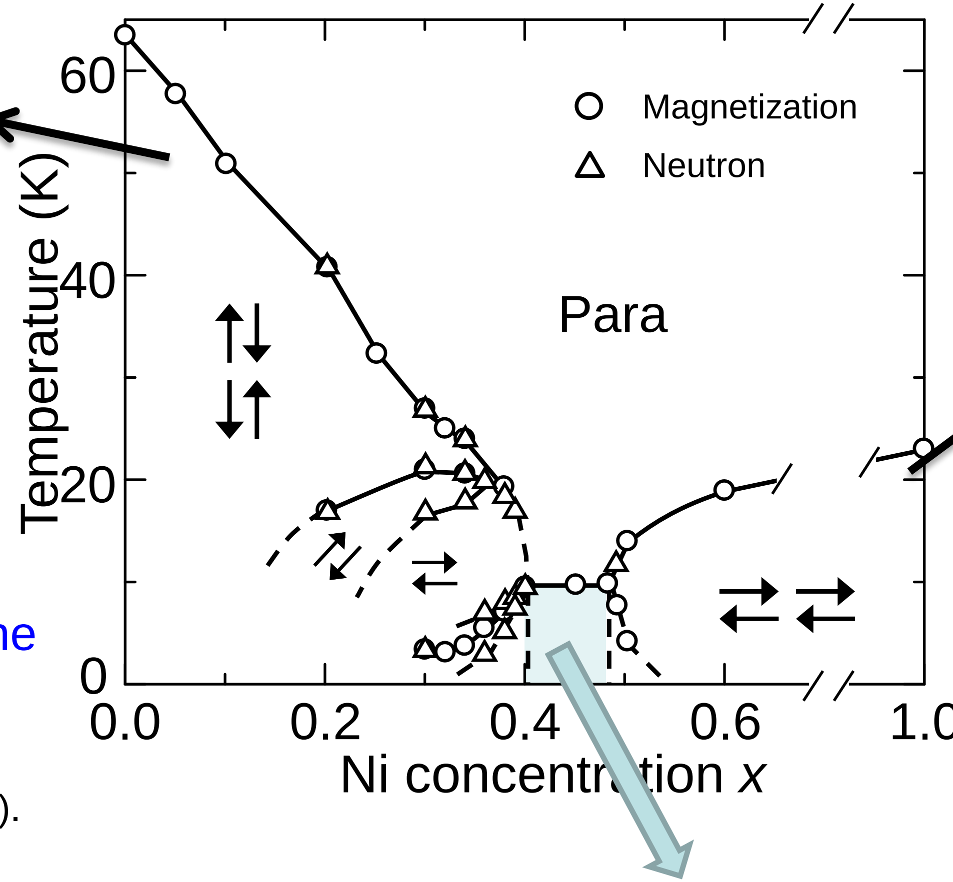

$NiTiO_3$

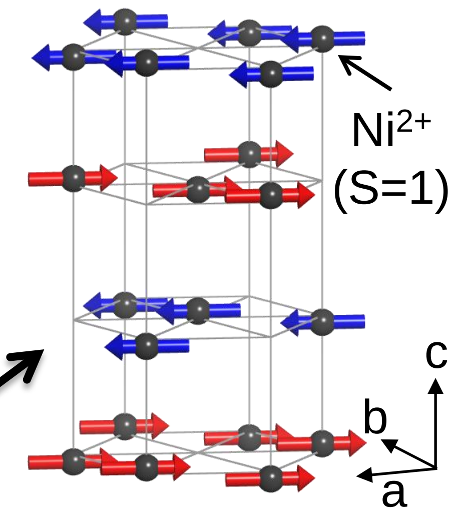

*AFM within *ab* plane
*eazy axis // *c* axis

G.Shirane *et al*.,
JPSJ 14, 1352 (1959).

*FM within *ab* plane
*AFM between layers
*easy axis // ab plane

- **$Ni_{1-x}Mn_xTiO_3$**

Both exchange interaction & magnetic anisotropy are randomly frustrated.

Ni = 0.4~0.5 shows spin glass phase with weak inplane anisotropy.

Magnetic & dielectric properties at zero magnetic fields

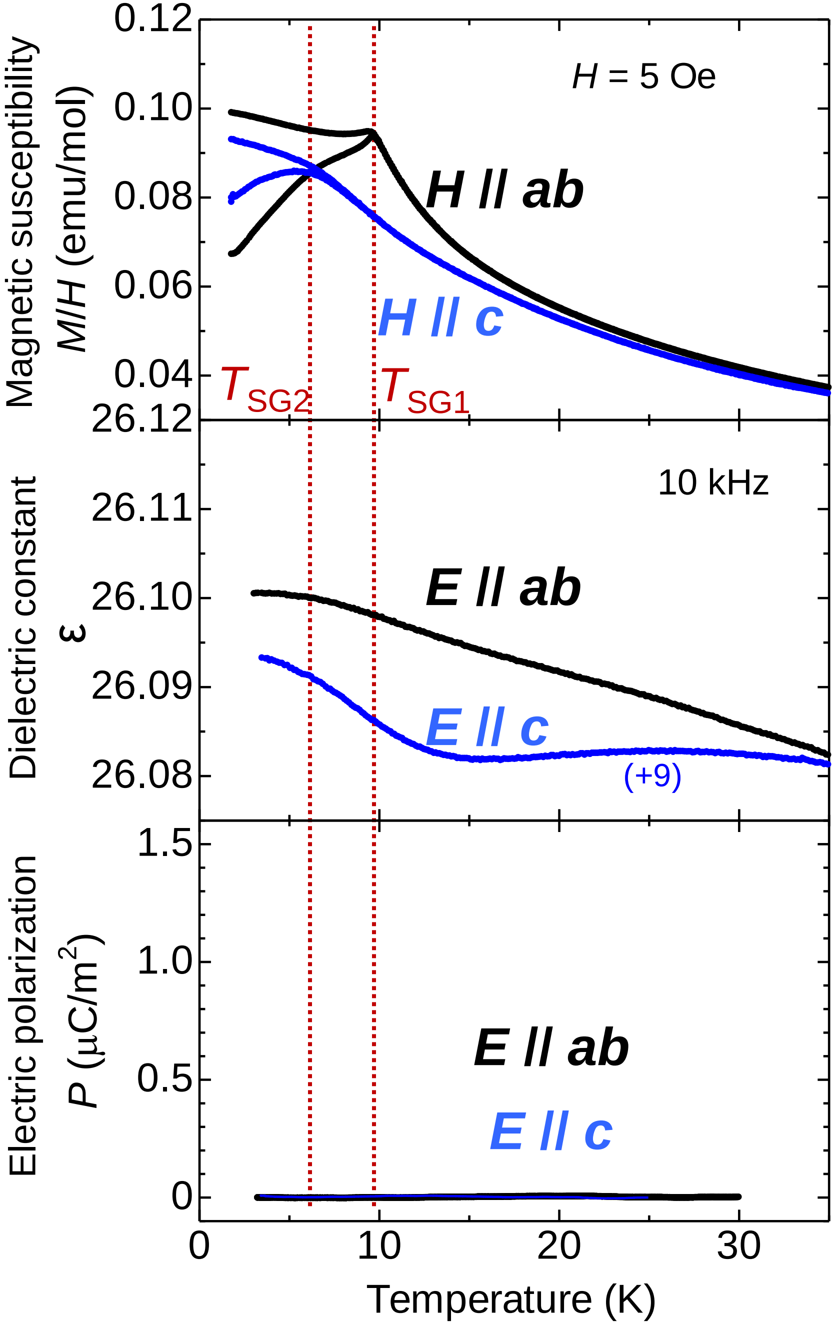

$Ni_{0.42}Mn_{0.58}TiO_3$

Magnetic susceptibility

Anomalies at T_{SG1} ~ 9.5 K

T_{SG2} ~ 6.0 K

Spin glass transition

[consistent with previous study

H. Kawano et al., JPSJ 62, 2575 (1993)]

Dielectric properties

No anomaly at T_{SG1} & T_{SG2}

No correlation between magnetic & dielectric properties was observed.

Magnetic field effect on electric polarization in $Ni_{0.42}Mn_{0.58}TiO_3$

Yamaguchi et al., PRL 108, 057203 (2012).

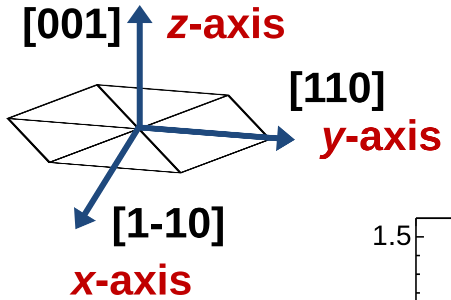

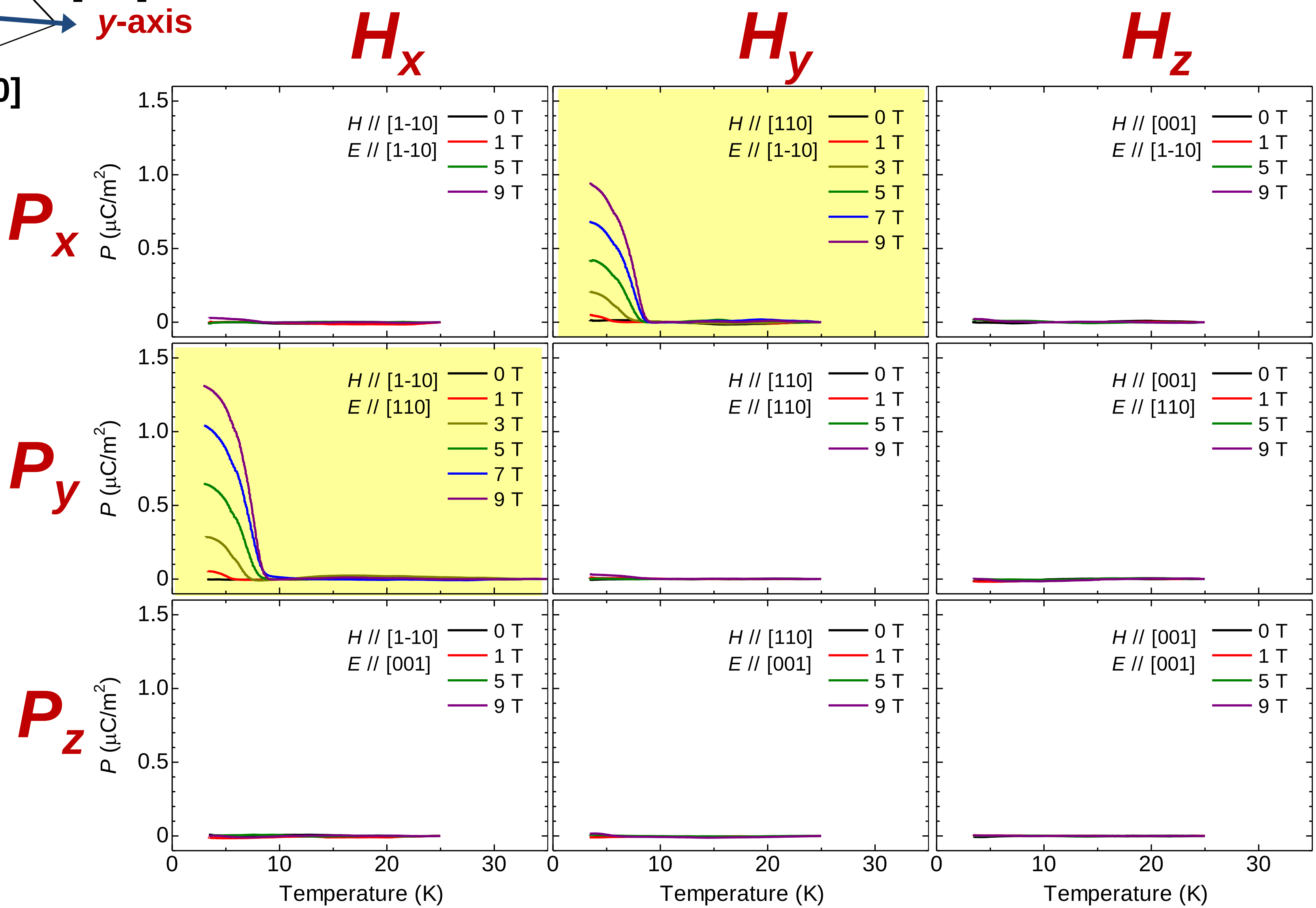

Antisymmetric ME effect induced by toroidal moment

Toroidal ordering induces ME effect

Toroidal moment *T*

ordered arrangement of magnetic vortices

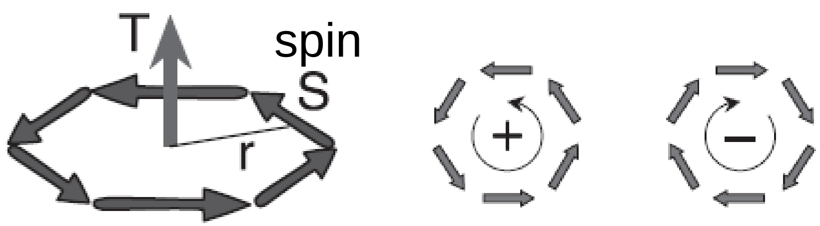

$$\boldsymbol{T} \sim \Sigma_\alpha \, \boldsymbol{r}_\alpha \times \boldsymbol{S}_\alpha$$

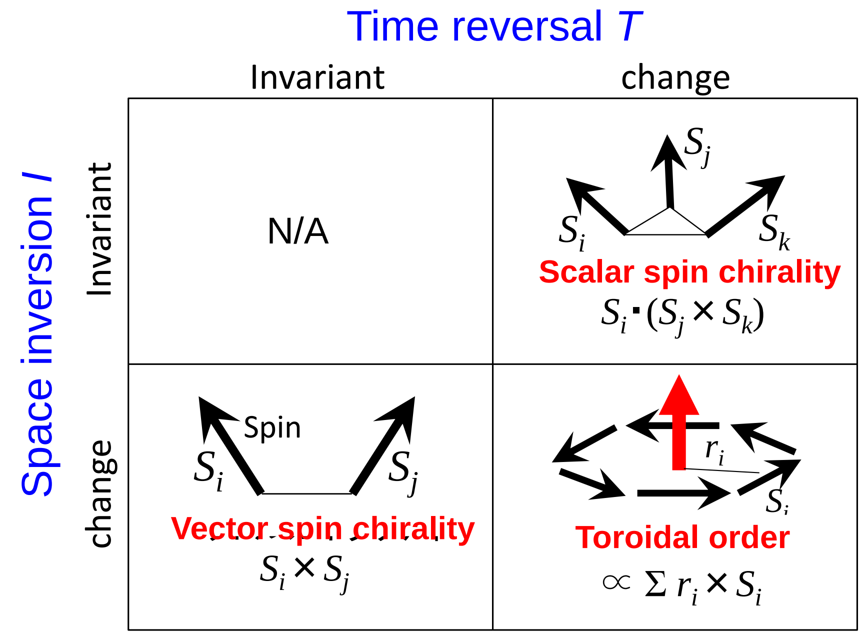

H. Schmid, J. Phys. Condens. Matter 20, 434203, 2008

<u>Free energy expression including toroidal moment ***T***</u>

term of toroidal moment   linear ME effect

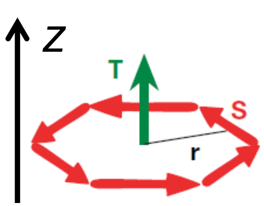

$$F = -P^s{}_i E_i - M^s{}_i H_i - T^s{}_i (\boldsymbol{E} \times \boldsymbol{H})_i \cdots - \alpha_{ij} E_i H_j \cdots$$

consider $\boldsymbol{T} = (0, 0, T_z)$

$$F = -P^s{}_i E_i - M^s{}_i H_i - T_z (E_x H_y - E_y H_x) \cdots - \alpha_{ij} E_i H_j \cdots$$

$$P_x = -\frac{\partial F}{\partial E_x} = P^s{}_x + \boldsymbol{T_z H_y} \cdots + \alpha_{xj} H_j \cdots \qquad P_y = -\frac{\partial F}{\partial E_y} = P^s{}_y - \boldsymbol{T_z H_x} \cdots + \alpha_{yj} H_j \cdots$$

off-diagonal & antisymmetric magnetoelectric effect

Summary - Study of Magnetoelectric Effects due to Multi-spin Variables -

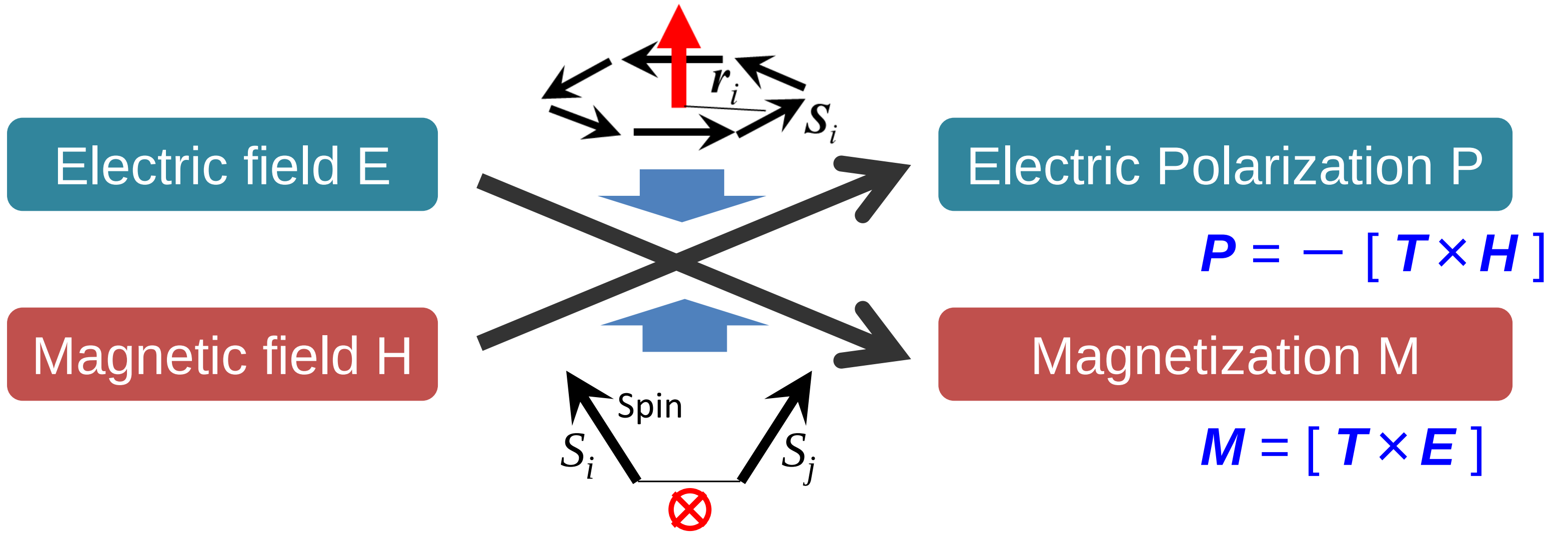

$$P = -[\,T \times H\,]$$

$$M = [\,T \times E\,]$$

Room-temperature magnetoelectrics possibly by spin spiral

Hexaferrites $Sr_3Co_2Fe_{24}O_{41}$ with the Z-type structure

Observation of spin-chiral domains in multiferroic hexaferrites by scanning resonant x-ray microdiffraction

Hexaferrites $Ba_{0.5}Sr_{1.5}Zn_2Fe_{12}O_{22}$ with the Y-type structure

Magnetoelectric effect observed in a magnetically-disordered system

XY-like spin-glass $(Ni,Mn)TiO_3$ with the ilmenite structure

Proposed work for synchrotron and neutron applications of high magnetic fields on multiferroics

$MnWO_4$

Spin-spiral multiferroic
with $P2/c$ monoclinic structure

Q_{mag}= (-0.214,1/2, 0.457)

Taniguchii et al. PRL 97, 097203 (2006)

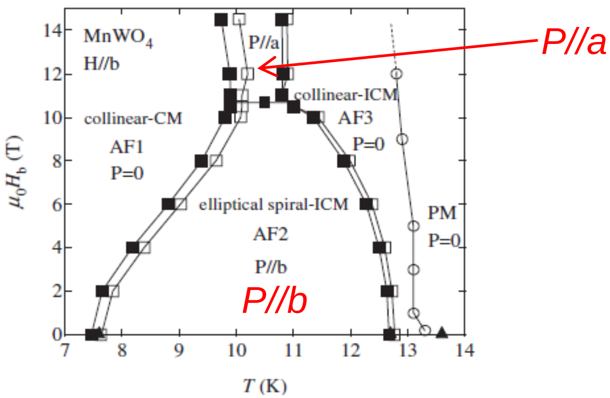

Nojiri et al. PRL 106, 237202 (2011)

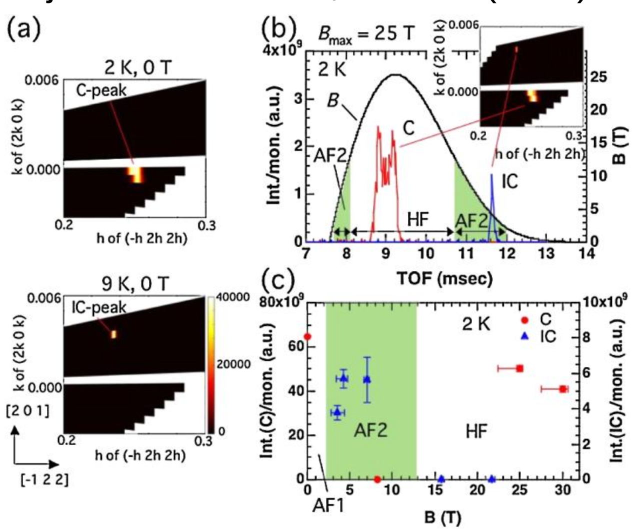

CuO

Spin-spiral multiferroic
with $C2/c$ monoclinic structure

Kimura *et al.*, Nature Mater. 7, 291 (2008)

Q_{mag}= (0.506,0,−0.483)

To be appeared in PRL

Magnetic Phase Diagram of CuO via High-Resolution Ultrasonic Velocity Measurements

R. Villarreal,[1] G. Quirion,[1] M. L. Plumer,[1] M. Poirier,[2] T. Usui,[3] and T. Kimura[3]
[1]*Department of Physics and Physical Oceanography, Memorial University, St. John's, Newfoundland, Canada A1B 3X7*
[2]*Département de Physique, Univesité de Sherbrooke, Sherbrooke, Québec, Canada J1K 2R1*
[3]*Division of Materials Physics, Osaka University, Toyonaka, Osaka, Japan*

(Received 22 May 2012; revised manuscript received 27 July 2012)

Experiment

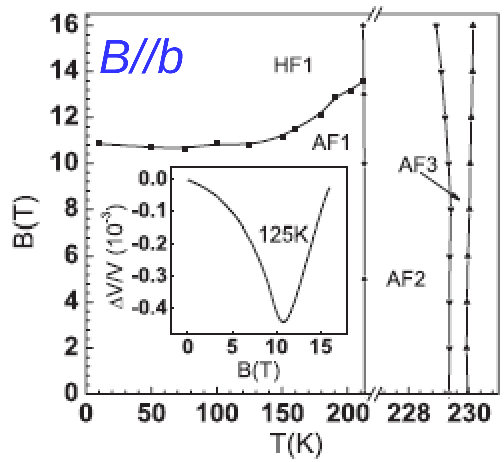

Theory

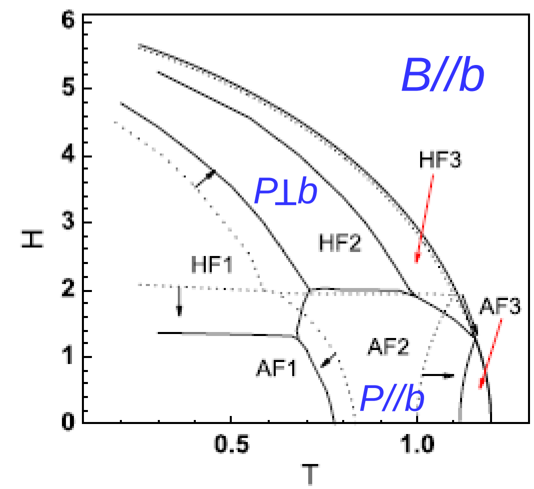

Landau-type free energy analysis suggests
a polarization flopped phase is induced by *B*.